frontiers in Molecular Biosciences

ORIGINAL RESEARCH
published: 04 February 2022
doi: 10.3389/fmolb.2021.801401

Phytochemicals of *Euphorbia hirta* L. and Their Inhibitory Potential Against SARS-CoV-2 Main Protease

Ruel Cayona and Evelyn Creencia**

Department of Chemistry, College of Science and Mathematics, Mindanao State University—Iligan Institute of Technology, Iligan, Philippines

Euphorbia hirta L. is a medicinal plant widely used in the Philippines and across tropical Asia against various diseases, including respiratory disorders. In this study, the phytochemical components of *E. hirta* were investigated *in silico* for their potential to inhibit the severe acute respiratory syndrome-coronavirus-2 main protease (SARS-CoV-2 Mpro), a coronavirus disease 2019 (COVID-19) drug target that plays a critical role in the infection process of SARS-CoV-2. Phytochemical mining in tandem with virtual screening (PM-VS) was the strategy implemented in this study, which allows efficient preliminary *in silico* assessment of the COVID-19 therapeutic potential of the reported phytochemicals from the plant. The main rationale for considering *E. hirta* in the investigation was its reported efficacy against respiratory disorders. It is very promising to investigate the phytochemicals of *E. hirta* for their potential efficacy against diseases, such as COVID-19, that also target the respiratory system. A total of 298 *E. hirta* phytochemicals were comprehensively collected from the scientific literature. One hundred seventy of these phytochemicals were computed through molecular docking and were shown to have comparable or better binding properties (promising inhibitors) toward SARS-CoV-2 Mpro than known *in vitro* inhibitors. In connection to our previous work considering different medicinal plants, antiviral compounds were also rediscovered from the phytochemical composition of *E. hirta*. This finding provides additional basis for the potential of the plant (or its phytochemicals) as a COVID-19 therapeutic directly targeting drug targets such as SARS-CoV-2 Mpro and/or addressing respiratory-system-related symptoms. The study also highlights the utility of PM-VS, which can be efficiently implemented in the preliminary steps of drug discovery and development.

Keywords: *Euphorbia hirta*, COVID-19, molecular docking, phytochemical mining, medicinal plant, Philippine medicinal plant, SARS-CoV-2 Mpro, virtual screening

OPEN ACCESS

Edited by:
Arvind Ramanathan, Argonne National Laboratory (DOE), United States

Reviewed by:
Debsindhu Bhowmik, Oak Ridge National Laboratory (DOE), United States
Lorane Hage-Melim, Universidade Federal do Amapá, Brazil

****Correspondence:***
Ruel Cayona
ruel.cayona@g.msuiit.edu.ph
Evelyn Creencia
evelyn.creencia@g.msuiit.edu.ph

Specialty section:
This article was submitted to Biological Modeling and Simulation, a section of the journal Frontiers in Molecular Biosciences

Received: *25 October 2021*
Accepted: *30 December 2021*
Published: *04 February 2022*

Citation:
Cayona R and Creencia E (2022) Phytochemicals of Euphorbia hirta *L. and Their Inhibitory Potential Against SARS-CoV-2 Main Protease. Front. Mol. Biosci. 8:801401. doi: 10.3389/fmolb.2021.801401*

1 INTRODUCTION

Euphorbia hirta L. (Euphorbiaceae) is a medicinal plant widely used in the Philippines and across tropical Asia, and it is commonly known by the following names: "asthma plant" (English), "tawa-tawa" (Filipino), and "mangagaw" (Cebuano). The extract of *E. hirta* is taken orally as an aqueous decoction for most of its folkloric uses. As its English common name suggests, the plant has been used for asthma and other respiratory difficulties (Ekpo and Pretorius, 2007; Ogunlesi et al., 2009; Rao et al., 2017). In addition, available studies conclusively suggest its potential against dengue

(Guzman et al., 2016; Perera et al., 2018; Suganthi and Ravi, 2018); however, additional studies are required to validate the results (Perera et al., 2018). Nevertheless, the studies reveal *E. hirta* as a pool for compounds with interesting biological activities.

E. hirta is one of the medicinal plants currently being investigated in the Philippines for its potential against coronavirus (CoV) disease 2019 (COVID-19) (Luci-Atienza, 2021a, Luci-Atienza, 2021b; Tawa-Tawa Clinical Trial on COVID-19, 2021). The goal is to develop a formulation utilizing the plant as an adjuvant treatment for mild to moderate COVID-19. A recently published review article identified *E. hirta* as one of the Philippine medicinal plants with immunomodulatory effects and potential against severe acute respiratory syndrome-CoV-2 (SARS-CoV-2) (Dayrit et al., 2021), the virus responsible for COVID-19. In this connection, a parallel and complementary *in silico* study was conducted to investigate the potential of its phytochemicals against a specific COVID-19 drug target, SARS-CoV-2 main protease (Mpro). Mpro is seen as an important COVID-19 drug target because of the role it plays in the regulation of viral replication (Di Micco et al., 2021).

It was the reported activities of *E. hirta* or its phytochemicals against respiratory-related ailments that serve as the primary basis for considering it as a subject of the present investigation. This study was conducted in line with the ongoing effort to discover potential COVID-19 therapeutic chemicals from medicinal plants, starting first with those found in the Philippines (Philippine medicinal plants). A strategy called phytochemical mining in tandem with virtual screening (PM-VS) was implemented. PM-VS refers to the systematic and comprehensive collection of medicinal plant phytochemicals reported in the scientific literature (phytochemical mining) and subsequent *in silico* assessment of the potential efficacy of the phytochemicals against specific or multiple drug target(s) (virtual screening). PM-VS and its rationale have been elaborated elsewhere (Cayona and Creencia, 2021a; Cayona and Creencia, 2021b, Cayona and Creencia, 2022). Specifically focused in this study is *E. hirta* and automated targeted molecular docking as the medicinal plant and virtual screening tool, respectively. It is argued that PM-VS can be efficiently implemented in the preliminary steps of drug discovery and development.

2 MATERIALS AND METHODS

2.1 Phytochemical Data Collection

The method implemented in this study is adapted from the method described in our previous papers (Cayona and Creencia, 2021a; Cayona and Creencia, 2021b) with slight modification. The Preferred Reporting Items for Systematic Reviews and Meta-analyses (PRISMA) (Moher et al., 2009) protocol was implemented throughout the systematic data collection process. The sources of phytochemicals were peer-reviewed research and review articles from scientific journals deposited in the MEDLINE database by the US National Institutes of Health National Library of Medicine (https://pubmed.ncbi.nlm.nih.gov/). The Google Scholar (https://scholar.google.com/) search engine was utilized to find additional literature but other search engines were also consulted (i.e., Microsoft Academic and Semantic Scholar), similarly applying relevant search keys and filters when applicable.

The identified sources were then compared against each other to check for multiple entries and reference-checked to retrieve additional sources unintentionally omitted in the first part of literature gathering. Articles deposited in restricted repositories and which were not written in English were not included. Thereafter, the phytochemicals reported in every literature reference were trimmed down to unique chemical identities only (because one compound may have multiple reported names). For simplicity, the common names of the compounds were taken in cases where ambiguity does not manifest; otherwise, the International Union of Pure and Applied Chemistry (IUPAC) nomenclature was adopted. The study strictly adhered to the data collection protocol described in PRISMA (see **Supplementary Materials**).

2.2 Phytochemical Classification

The collected phytochemicals from *E. hirta* were classified according to the ClassyFire (Djoumbou Feunang et al., 2016) algorithm of chemical classification. This was done to gain insight that might be helpful in assessing the basic structure–activity relationship. The hierarchy of chemical taxonomic classification can be found in the **Supplementary Materials**.

2.3 Preparation of Ligands

Three-dimensional (3D) structure-data files (SDFs) of phytochemicals included in the final list were either conveniently collected from PubChem or manually generated whenever they are unavailable in the database. Hydrogen atoms were explicitly added to the structures. In some cases, two-dimensional (2D) SDFs were used but only for 2D compounds (linear or flat). In preparation for virtual screening and for future convenience, the SDFs of all the structures of the phytochemicals (the ligands) were combined into a single SDF using OpenBabel 2.4.1 (O'Boyle et al., 2011) to facilitate automated importing of the multiple structures into the virtual screening tool. The same preparation was done for the control compounds.

2.4 Receptor Preparation

The crystal structure at 2.16 Å of the SARS-COV-2 Mpro (PDB ID: 6LU7) in complex with the *in vitro* inhibitor N3 (Jin et al., 2020) was downloaded from the Protein Data Bank (http://www.rcsb.org/) in a PDB file format. The noninteracting atoms (e.g., water and buffer molecules) were removed, and hydrogen atoms were explicitly added to the enzyme and the native ligand.

The active site was taken as the region of the SARS-CoV-2 Mpro volume where the *in vitro* inhibitor N3 was attached. From the SARS-CoV-2 Mpro–N3 complex, the search space for the targeted molecular docking was then assigned with the help of BIOVIA Discovery Studio Visualizer v20.1.0.19295 (DSV, 2020). The interacting and the pocket amino acids (AAs) that lie within the 3.5 Å distance from the closest N3 atom were identified by

visual inspection. The residues found within this region totaled 25 AAs. The interacting AAs were H41, M49, F140, N142, G143, H164, M165, E166, L167, P168, H172, Q189, T190, and T191; and the pocket AAs were T24, T25, T26, L27, Y54, L141, S144, C145, H163, D187, R188, and Q192. From this list of AAs, the H41–C145 catalytic dyad can be found (Wang YC. et al., 2020; Hakmi et al., 2020; Ullrich and Nitsche, 2020).

2.5 Virtual Screening Through Automated Molecular Docking

2.5.1 Molecular Docking Tools

The phytochemical ligands were virtually screened against SARS-CoV-2 Mpro (6LU7-neat) using PyRx0.8 (Dallakyan and Olson, 2015), a virtual screening tool that allows automated molecular docking of multiple ligands (or libraries) against target receptor (s). PyRx0.8 utilizes the enabling capabilities of AutoDock tools for receptor and ligand preparation just as in AutoDock 4 (Morris et al., 2009) and the earlier versions; AutoDock Vina for molecular docking (Trott and Olson, 2010); OpenBabel for file format interconversion (O'Boyle et al., 2011); and other open-source software. To save on computational cost, targeted molecular docking on the active site of Mpro was conducted.

2.5.2 Control Parameters

To enhance the accuracy, control parameters were set in molecular docking against Mpro. In addition to the phytochemical ligands, control ligand samples were also tested. Ten known inhibitors with established *in vitro* half-maximal effective concentration (EC_{50}) against SARS-CoV-2 or half-maximal inhibitory concentration (IC_{50}) against SARS-CoV-2 Mpro were used as positive controls. On the other hand, 10 small molecules that do not possess interesting pharmacological properties were also used as negative controls. The positive controls were N3 (6LU7 native ligand), efonidipine, bedaquiline, tideglusib, manidipine, N3, lercanidipine, boceprevir, shikonin, ebselen, and carmofur, whose inhibitory properties were reported elsewhere (Ghahremanpour et al., 2020; Jin et al., 2020; Ma et al., 2020). The negative controls chosen were anthracene, naphthalene, glycerol, decane, hexanol, benzene, cyclohexane, hexane, ethanol, and water. The positive controls (inhibitors) were expected to give satisfactory binding free energy (BFE) values towards the receptor SARS-CoV-2 Mpro because they are empirically established inhibitors. On this basis, their BFEs were taken as a reference in assigning promising phytochemicals against SARS-CoV-2 Mpro. In contrast, the negative controls should have unsatisfactory computed BFE towards the receptor. The control ligands provide a simple means to assess the reliability and performance of the virtual screening tool.

2.5.3 Automated Molecular Docking

The receptor (6LU7-neat) was loaded onto PyRx0.8 and set into the macromolecule (receptor) in the PDBQT format. The collective SDFs of the phytochemicals and positive and negative controls previously prepared using OpenBabel 2.4.1 were also loaded onto PyRx0.8 and subsequently extracted automatically to individual structures. The structures were then energy minimized by implementing suitable force fields. For most of the structures, MMFF94 was sufficient in energy minimization; however, UFF and/or Ghemical must be implemented for some ligands whose final structures were distorted under specified UFF minimization parameters. Thereafter, the ligands were converted into a docking-ready PDBQT file format.

Before docking, the search space for the targeted automated molecular docking was set. The interacting and the pocket AA residues of SARS-CoV-2 Mpro that were identified previously were selected, and the search space was adjusted manually in the PyRx0.8 interface so that all of the residues were included in the grid volume of the search space. The resulting grid dimensions are the following: center_x = −10.8864; center_y = 14.0407; center_z = 68.7458; size_x = 21.4856; size_y = 26.7715; size_z = 28.0882. The exhaustiveness of the most stable conformation search was set at 16. Finally, docking was commenced using the Vina (AutoDock Vina) tab in PyRx0.8.

2.5.4 Receptor–Ligand Interaction Analysis

Interactions of the ligands which have BFEs comparable to or better than those of the positive controls were analyzed. Those ligands whose most stable binding conformation (docking RMSD = 0) established interactions with the H41–C145 catalytic dyad (Jin et al., 2020; Khan et al., 2020; Menéndez et al., 2020; Mirza and Froeyen, 2020; Shitrit et al., 2020) of the SARS-CoV-2 Mpro and those with reported antiviral properties were given emphasis. Favorable computed BFE and catalytic dyad interaction(s) were considered as major criteria in identifying promising SARS-CoV-2 Mpro inhibitors.

2.5.5 Assessment of the Reliability of the Tools and Strategies

All the tools and strategies used in the study are well established throughout the scientific literature. The number of citations of the articles that report the tools and strategies partly establish their reputation in the field. For example, Google Scholar queries on PRISMA, ClassyFire, PyRx0.8, AutoDock Vina, and AutoDock 4 will reveal 7,156; 283; 873; 15,275; and 12,351 citations, respectively, as of July 17, 2021.

3 RESULTS

3.1 Phytochemical Mining and Classification

Literature reports indicate that leaves, aerial parts, and whole plants are the sources of *E. hirta* phytochemicals. The relevant data collected from phytochemical mining (PM) *E. hirta* are presented in **Table 1**. Each phytochemical is provided with its molecular formula (MF), BFE value against SARS-CoV-2 Mpro, and chemical taxonomy grouping levels (ClassyFire Superclass, Class, and Subclass). The chemical structures of all *E. hirta* phytochemicals and the control samples (positive and negative) used in molecular docking can be found in the **Supplementary Materials**. In total, 298 phytochemical

TABLE 1 | Phytochemicals from *E. hirta*.

ID	Phytochemical	MF[a]	BFE[b]
	Benzenoids/benzene and substituted derivatives		
1	1-(3-aminophenyl)ethanol (Rautela et al.,2020)	$C_8H_{11}NO$	−4.6
2	1-*O*-butyl 2-*O*-tetradecyl benzene-1,2-dicarboxylate (Ogunlesi et al.,2009)	$C_{26}H_{42}O_4$	−4.9
3	benzoic acid (Ali et al.,2020)	$C_7H_6O_2$	−4.5
4	benzamide, 3-fluoro-*N*-butyl-*N*-ethyl (Rautela et al.,2020)	$C_{13}H_{18}FNO$	−4.9
5	gallic acid (Bach et al.,2020; Linfang et al., 2012; Mahomoodally et al.,2020; Mekam et al.,2019, Suganthi and Ravi, 2018; Wu et al.,2012)	$C_7H_6O_5$	−5.5
6	ethyl gallate (Mekam et al.,2019)	$C_9H_{10}O_5$	−5.7
7	methyl gallate (Mahomoodally et al.,2020)	$C_8H_8O_5$	−5.6
8	protocatechuic acid (Mahomoodally et al.,2020)	$C_7H_6O_4$	−5.4
9	1-(3-ethoxyphenyl)propan-2-one (Rautela et al.,2020)	$C_{11}H_{14}O_2$	−5.0
10	methyl 3-(3,5-di-*tert*-butyl-4-hydroxyphenyl)propanoate (Perumal and Mahmud, 2013)	$C_{18}H_{28}O_3$	−6.5
	Benzenoid/naphthalene		
11	[6-(4-cyanophenyl)naphthalen-2-yl] hexanoate (Rautela et al.,2020)	$C_{23}H_{21}NO_2$	−6.5
	Benzenoids/phenols		
12	benzene-1,2,3-triol (Karki et al.,2019)	$C_6H_6O_3$	−4.9
13	2-*tert*-butyl-4-methoxyphenol (Rautela et al.,2020)	$C_{11}H_{16}O_2$	−5.1
14	4-ethenyl-2-methoxyphenol (Rautela et al.,2020)	$C_9H_{10}O_2$	−4.7
	Benzenoid		
15	1,2-benzenedicarboxylic acid diisooctyl ester (Ogunlesi et al.,2009)	$C_{24}H_{38}O_4$	−5.4
	Hydrocarbon/saturated hydrocarbon		
16	Tetradecane (Ogunlesi et al.,2009)	$C_{14}H_{30}$	−4.2
	Hydrocarbon/unsaturated hydrocarbon		
17	(*E*)-pentatriacont-17-ene (Rautela et al.,2020)	$C_{35}H_{70}$	−4.4
	Lignans, neolignans, and related compounds/aryltetralin lignans		
18	Isolintetralin (Zhang et al.,2020)	$C_{23}H_{28}O_6$	−7.1
19	Lintetralin (Zhang et al.,2020)	$C_{23}H_{28}O_6$	−7.3
20	Phyltetralin (Zhang et al.,2020)	$C_{24}H_{32}O_6$	−7.0
21	Hypophyllanthin (Zhang et al.,2020)	$C_{24}H_{30}O_7$	−6.9
	Lignans, neolignans, and related compounds/dibenzylbutane lignans		
22	Niranthin (Zhang et al.,2020)	$C_{24}H_{32}O_7$	−6.3
23	5-demethoxyniranthin (Zhang et al.,2020)	$C_{23}H_{30}O_6$	−6.3
24	Phyllanthin (Zhang et al.,2020)	$C_{24}H_{34}O_6$	−5.9
	Lignans, neolignans, and related compounds/furanoid lignans		
25	Virgatusin (Zhang et al.,2020)	$C_{23}H_{28}O_7$	−6.4
26	Urinaligran (Zhang et al.,2020)	$C_{22}H_{24}O_7$	−7.4
27	7-hydroxyhinokinin (Zhang et al.,2020)	$C_{20}H_{18}O_8$	−8.2
28	(−)-pinoresinol (Li et al.,2015)	$C_{20}H_{22}O_6$	−7.2
29	(+)-syringaresinol (Li et al.,2015)	$C_{22}H_{26}O_8$	−7.6
	Lignans, neolignans, and related compounds/lignan glycosides		
30	(+)-syringaresinol glucoside (Li et al.,2015)	$C_{28}H_{36}O_{13}$	−7.0
31	(−)-pinoresinol glucoside (Li et al.,2015)	$C_{26}H_{32}O_{11}$	−7.6
	Lignans		
32	5-methoxyvirgatusin (Zhang et al.,2020)	$C_{24}H_{30}O_8$	−7.2
33	7R-ethoxy-3-methoxyisolintetralin (Zhang et al.,2020)	$C_{26}H_{34}O_8$	−6.7
34	7R-ethoxyisolintetralin (Zhang et al.,2020)	$C_{25}H_{32}O_7$	−6.8
35	7S-ethoxyisolintetralin (Zhang et al.,2020)	$C_{25}H_{32}O_7$	−7.6
36	chebulic acid triethyl ester (Yang et al.,2020)	$C_{20}H_{24}O_{11}$	−6.2
37	euphorhirtin A (Yang et al.,2020; Zhang et al.,2020)	$C_{19}H_{20}O_{11}$	−6.5
38	euphorhirtin B (Yang et al.,2020; Zhang et al.,2020)	$C_{19}H_{20}O_{11}$	−6.6
39	euphorhirtin C (Yang et al.,2020; Zhang et al.,2020)	$C_{18}H_{18}O_{11}$	−6.6
40	euphorhirtin D (Yang et al.,2020; Zhang et al.,2020)	$C_{18}H_{18}O_{11}$	−6.8
41	hirtacoumaroflavonoside (Sheliya et al.,2015)	$C_{41}H_{44}O_{17}$	−8.7
42	hirtacoumaroflavonoside B (Sheliya et al.,2015)	$C_{31}H_{36}O_{12}$	−8.4
43	Neonirtetralin (Zhang et al.,2020)	$C_{20}H_{22}O_7$	−6.7
44	3,5-*O*-dicaffeoylquinic acid (Mekam et al.,2019)	$C_{25}H_{24}O_{12}$	−9.2
	Lipids and lipid-like molecules/fatty acyls		
45	2-(dimethylamino)ethyl 3-cyclopentylpropanoate (Rautela et al.,2020)	$C_{12}H_{23}NO_2$	−4.8
46	3-octadecoxypropyl (*Z*)-octadec-9-enoate (Karki et al.,2019)	$C_{39}H_{76}O_3$	−4.2
47	ethyl hexadecanoate (Sharma et al.,2014)	$C_{18}H_{36}O_2$	−4.4
48	ethyl octadecanoate (Sharma et al.,2014)	$C_{20}H_{40}O_2$	−4.4
49	methyl (11*E*,14*E*,17*E*)-icosa-11,14,17-trienoate (Karki et al.,2019)	$C_{21}H_{36}O_2$	−4.9
50	methyl 9-octadecanoate (Olaoluwa et al.,2018)	$C_{19}H_{36}O_2$	−4.3
51	methyl hexadecanoate (Perumal and Mahmud, 2013; Olaoluwa et al.,2018; Karki et al.,2019; Rautela et al.,2020)	$C_{17}H_{34}O_2$	−4.3

(Continued on following page)

TABLE 1 | (*Continued*) Phytochemicals from *E. hirta*.

ID	Phytochemical	MF[a]	BFE[b]
52	citronellyl palmitoleate (Rautela et al.,2020)	$C_{26}H_{48}O_2$	−5.0
53	geranyl linoleate (Rautela et al.,2020)	$C_{28}H_{48}O_2$	−5.2
54	(*Z*)-3,7-dimethylocta-2,6-dien-1-yl palmitate (Rautela et al.,2020)	$C_{26}H_{48}O_2$	−5.4
55	oleic acid (Ogunlesi et al.,2009)	$C_{18}H_{34}O_2$	−5.0
56	pentadecanoic acid (Sharma et al.,2014)	$C_{15}H_{30}O_2$	−4.8
57	tetradecanoic acid (Sharma et al.,2014)	$C_{14}H_{28}O_2$	−4.5
58	hexadecanoic acid (Ogunlesi et al.,2009; Perumal and Mahmud, 2013; Rautela et al.,2020)	$C_{16}H_{32}O_2$	−4.4
59	methyl 3-hydroxyoctanoate *O*-beta-D-glucopyranoside (Nomoto et al.,2013)	$C_{15}H_{28}O_8$	
60	*N*-butyl-1-*O*-alpha-L-rhamnopyranoside (Mallavadhani and Narasimhan, 2009)	$C_{10}H_{20}O_5$	−5.2
61	*N*-butyl-1-*O*-beta-L-rhamnopyranoside (Mallavadhani and Narasimhan, 2009)	$C_{10}H_{20}O_5$	−5.4
62	sodium beta-D-glucopyranosyl 12-hydroxyjasmonate (*acid form was used in docking) (Bach et al.,2020)	$C_{18}H_{28}O_9$	−7.0
63	bumaldoside A (Nomoto et al.,2013)	$C_{19}H_{36}O_{10}$	−7.2
64	byzantionoside B (Nomoto et al.,2013)	$C_{19}H_{32}O_7$	−7.1
65	corchoionoside C (Nomoto et al.,2013)	$C_{19}H_{30}O_8$	−7.2
66	Roseoside (Mekam et al.,2019)	$C_{19}H_{30}O_8$	−7.0
67	(*Z*)-3-hexenyl-beta-D-glucopyranoside (Nomoto et al.,2013)	$C_{12}H_{22}O_6$	−6.3
68	geranyl acetate (Rautela et al.,2020)	$C_{12}H_{20}O_2$	−5.0
69	neryl acetate (Rautela et al.,2020)	$C_{12}H_{20}O_2$	−4.9
70	(9*E*,12*E*,15*E*)-octadeca-9,12,15-trien-1-ol (Sharma et al.,2014)	$C_{18}H_{32}O$	−4.7
71	heptadec-13-yn-1-ol (Ogunlesi et al.,2009)	$C_{17}H_{32}O$	−4.4
72	(*Z*)-octadec-13-enal (Karki et al.,2019)	$C_{18}H_{34}O$	−4.1
73	(*Z*)-tetradec-9-enal (Karki et al.,2019)	$C_{14}H_{26}O$	−4.5
74	hexadecanal (Ogunlesi et al.,2009)	$C_{16}H_{32}O$	−4.2
75	(*Z*)-octadec-9-enamide (Olaoluwa et al.,2018)	$C_{18}H_{35}NO$	−4.2
76	tetradecanamide (Olaoluwa et al.,2018)	$C_{14}H_{29}NO$	−4.5
77	(1′,*R*,5′*R*)-5-(5′-carboxymethyl-2′-oxocyclopentyl)-3-*Z*-pentenyl acetate (Chi et al.,2012)	$C_{14}H_{20}O_5$	
78	methyl linolenate (Perumal and Mahmud, 2013; Rautela et al.,2020)	$C_{19}H_{32}O_2$	−5.2
79	methyl linoleate (Rautela et al.,2020; Sharma et al.,2014)	$C_{19}H_{34}O_2$	−4.4
80	glyceryl monolinoleate (Rautela et al.,2020)	$C_{21}H_{38}O_4$	−5.1
81	ethyl linoleate (Rautela et al.,2020; Sharma et al.,2014)	$C_{20}H_{36}O_2$	−4.4
82	linolenic acid (Rautela et al.,2020)	$C_{18}H_{30}O_2$	−4.9
83	linoleic acid (Perumal and Mahmud, 2013)	$C_{18}H_{32}O_2$	−4.6
	Lipids and lipid-like molecules/glycerolipids		
84	2,3-dihydroxypropyl octadecanoate (Rautela et al.,2020)	$C_{21}H_{42}O_4$	−4.5
85	2-monopalmitin (Perumal and Mahmud, 2013; Rautela et al.,2020)	$C_{19}H_{38}O_4$	−4.7
86	2-monostearin (Perumal and Mahmud, 2013)	$C_{21}H_{42}O_4$	−4.7
87	triolein (Karki et al.,2019)	$C_{57}H_{104}O_6$	−4.5
	Lipids and lipid-like molecules/prenol lipids/diterpenoids		
88	(*E*)-3,7,11,15-tetramethylhexadec-2-en-1-ol (Ogunlesi et al.,2009)	$C_{20}H_{40}O$	−5.2
89	phytol (Ogunlesi et al.,2009; Perumal and Mahmud, 2013; Sharma et al.,2014; Olaoluwa et al.,2018; Karki et al.,2019)	$C_{20}H_{40}O$	−5.1
90	gibberellin (Mekam et al.,2019)	$C_{20}H_{28}O_6$	−6.2
91	ponicidin (Mekam et al.,2019)	$C_{20}H_{26}O_6$	−7.5
92	albopilosin H (Mekam et al.,2019)	$C_{20}H_{28}O_4$	−6.5
93	kaur-16-ene (Olaoluwa et al.,2018)	$C_{20}H_{32}$	−6.6
	Lipids and lipid-like molecules/prenol lipids/monoterpenoids		
94	(*E*)-3,7-dimethyl-2,6-octadienoic acid (Rautela et al.,2020)	$C_{10}H_{16}O_2$	−4.7
95	citronellol (Rautela et al.,2020)	$C_{10}H_{20}O$	−4.5
96	camphol (Shah et al.,2019)	$C_{10}H_{18}O$	−4.3
97	*cis*-alpha-bergamotene (Rautela et al.,2020)	$C_{15}H_{24}$	−5.0
98	2,6,6-trimethylbicyclo[3.1.1]heptane-2,3-diol (Rautela et al.,2020)	$C_{10}H_{18}O_2$	−4.9
99	*para*-menth-3-en-9-ol (Olaoluwa et al.,2018)	$C_{10}H_{18}O$	−4.9
100	tricyclo[4.2.2.01,5]decan-3-ol (Rautela et al.,2020)	$C_{10}H_{16}O$	−4.8
	Lipids and lipid-like molecules/prenol lipids/quinone and hydroquinone lipids		
101	gamma-tocopherol (Rautela et al.,2020; Sharma et al.,2014)	$C_{28}H_{48}O_2$	−6.2
102	vitamin E (Perumal and Mahmud, 2013; Rautela et al.,2020)	$C_{29}H_{50}O_2$	−6.7
	Lipids and lipid-like molecules/prenol lipids/sesquiterpenoids		
103	isospathulenol (Rautela et al.,2020)	$C_{15}H_{24}O$	−5.9
104	beta-elemene (Olaoluwa et al.,2018)	$C_{15}H_{24}$	−5.0
105	neointermedeol (Rautela et al.,2020)	$C_{15}H_{26}O$	−5.5
106	germacren D-4-ol (Rautela et al.,2020)	$C_{15}H_{26}O$	−5.6
107	beta-bisabolene (Rautela et al.,2020)	$C_{15}H_{24}$	−5.7
108	*cis*-nerolidol (Rautela et al.,2020)	$C_{15}H_{26}O$	−5.3
109	alpha-humulene (Rautela et al.,2020)	$C_{15}H_{24}$	−4.9
110	alpha-farnesene (Rautela et al.,2020)	$C_{15}H_{24}$	−5.2

(Continued on following page)

TABLE 1 | (*Continued*) Phytochemicals from *E. hirta*.

ID	Phytochemical	MF[a]	BFE[b]
111	beta-caryophyllene (Olaoluwa et al.,2018); Rautela et al.,2020)	$C_{15}H_{24}$	−5.1
112	farnesol 1 (Rautela et al.,2020)	$C_{15}H_{26}O$	−5.2
113	2,6,10-trimethyltetradecane (Ogunlesi et al.,2009)	$C_{17}H_{36}$	−4.3
114	neophytadiene (Perumal and Mahmud, 2013; Rautela et al.,2020)	$C_{20}H_{38}$	−4.6
115	6,10,14-trimethylpentadecan-2-one (Ogunlesi et al.,2009; Perumal and Mahmud, 2013)	$C_{18}H_{36}O$	−5.0
116	taraxerol acetate (Li et al.,2015)	$C_{32}H_{52}O_2$	−7.5
117	taraxerone (Ragasa and Cornelio, 2013; Li et al.,2015; Tayone et al.,2020)	$C_{30}H_{48}O$	−8.0
118	taraxerol (Perumal and Mahmud, 2013; Prachi and Pradeep, 2014; Li et al.,2015; Amos Samkumar et al.,2019; Bach et al.,2020; Tayone et al.,2020)	$C_{30}H_{50}O$	−7.8
	Lipids and lipid-like molecule/terpene glycoside		
119	citroside A (Nomoto et al.,2013)	$C_{19}H_{30}O_8$	−6.8
	Lipids and lipid-like molecule/triterpenoids		
120	friedelane-3beta,29-diol (Li et al.,2015)	$C_{30}H_{52}O_2$	−7.6
121	psi-taraxastane-3,20-diol (Li et al.,2015)	$C_{30}H_{52}O_2$	−7.4
122	squalene (Perumal and Mahmud, 2013; Sharma et al.,2014)	$C_{30}H_{50}$	−5.4
123	lanost-8-en-3beta-ol (Rautela et al.,2020)	$C_{30}H_{52}O$	−6.1
124	lupeol (Ragasa and Cornelio, 2013; Tayone et al.,2020)	$C_{30}H_{50}O$	−7.3
125	friedelan-3beta-ol (Li et al.,2015)	$C_{30}H_{52}O$	−7.9
126	friedelin (Linfang et al., 2012; Li et al.,2015)	$C_{30}H_{50}O$	−8.2
127	alpha-amyrin (Linfang et al., 2012; Perumal and Mahmud, 2013; Ragasa and Cornelio, 2013)	$C_{30}H_{50}O$	−7.9
128	beta-amyrin (Martínez-Vázquez et al.,1999; Perumal and Mahmud, 2013; Ragasa and Cornelio, 2013)	$C_{30}H_{50}O$	−7.2
	Lipids and lipid-like molecules/steroids and steroid derivatives/cycloartanols and derivatives		
129	(23*E*)-cycloart-23-en-3beta,25-diol (Tayone et al.,2020)	$C_{30}H_{50}O_2$	−7.0
130	cycloart-23-ene-3beta,25,28-triol (Li et al.,2015)	$C_{30}H_{50}O_3$	−6.8
131	cyclolanostan-3beta-ol (Li et al.,2015)	$C_{30}H_{52}O$	−6.7
132	24-hydroperoxycycloart-25-en-3beta-ol (Ragasa and Cornelio, 2013; Tayone et al.,2020)	$C_{30}H_{50}O_3$	−7.3
133	25-hydroperoxycycloart-23-en-3beta-ol (Ragasa and Cornelio, 2013; Tayone et al.,2020)	$C_{30}H_{50}O_3$	−8.0
134	cycloart-23-ene-3beta,25-diol (Li et al.,2015)	$C_{30}H_{50}O_2$	−7.1
135	cycloartenol (Perumal and Mahmud, 2013; Ragasa and Cornelio, 2013; Li et al.,2015)	$C_{30}H_{50}O$	−6.9
	Lipids and lipid-like molecule/steroids and steroid derivative/ergostane steroids		
136	campesterol (Perumal and Mahmud, 2013; Bach et al.,2020; Rautela et al.,2020)	$C_{28}H_{48}O$	−6.9
	Lipids and lipid-like molecule/steroids and steroid derivative/stigmastanes and derivatives		
137	stigmasterol (Rautela et al.,2020)	$C_{29}H_{48}O$	−7.1
138	gamma-sitosterol (Perumal and Mahmud, 2013; Rautela et al.,2020)	$C_{29}H_{50}O$	−6.8
139	beta-sitosterol (Martínez-Vázquez et al.,1999; Mallavadhani and Narasimhan, 2009; Tayone et al.,2020)	$C_{29}H_{50}O$	−6.8
140	16alpha,17-dihydroxy-ent-kaurane-3-one (Li et al.,2015)	$C_{20}H_{32}O_3$	−7.9
141	16alpha,17,19-trihydroxy-ent-kaurane (Li et al.,2015)	$C_{20}H_{34}O_3$	−6.5
142	16alpha,19-dihydroxy-ent-kaurane (Yan et al.,2011)	$C_{20}H_{34}O_2$	−6.1
143	16beta,17-dihydroxy-ent-kaurane-3-one (Li et al.,2015)	$C_{20}H_{32}O_3$	−7.0
144	23(*E*)-25-methoxycycloart-23-en-3beta-ol (Li et al.,2015)	$C_{31}H_{52}O_2$	−7.7
145	24-methylencycloartenol (Martínez-Vázquez et al.,1999)	$C_{29}H_{50}O$	−7.1
146	28-hydroxyfriedelin (Li et al.,2015)	$C_{30}H_{50}O_2$	−7.7
147	2beta,16alpha,19-trihydroxy-ent-kaurane (Li et al.,2015; Yan et al.,2011)	$C_{20}H_{34}O_3$	−6.3
148	3beta,16alpha,17-trihydroxy-ent-kaurane (Li et al.,2015)	$C_{20}H_{34}O_3$	−6.9
149	3beta-hydroxy-cycloart-25-ene-24-one (Li et al.,2015)	$C_{30}H_{48}O_2$	−6.5
150	3beta-hydroxyurs-12-ene (Mallavadhani and Narasimhan, 2009)	$C_{29}H_{48}O$	−7.7
151	ent-kaur-16-ene-3beta-ol (Li et al.,2015)	$C_{21}H_{34}$	−6.4
152	isojaponin A (Mekam et al.,2019)	$C_{21}H_{30}O_6$	−7.5
	Organic 1,3-dipolar compound/allyl-type 1,3-dipolar organic compound		
153	azidocyclohexane (Rautela et al.,2020)	$C_6H_{11}N_3$	−4.3
	Organic acids and derivatives/carboxylic acids and derivatives		
154	ethyl 1-ethylpyrrolidine-2-carboxylate (Rautela et al.,2020)	$C_9H_{17}NO_2$	−4.4
155	phenylalanine (Mekam et al.,2019)	$C_9H_{11}NO_2$	−5.3
156	tyrosine (Mekam et al.,2019)	$C_9H_{11}NO_3$	−5.5
157	2-[[2-amino-3-(4-hydroxyphenyl)propanoyl]amino]pentanedioic acid (Mekam et al.,2019)	$C_{14}H_{18}N_2O_6$	−6.8
158	maleic acid (Linfang et al., 2012)	$C_4H_4O_4$	−4.3
159	dehydrochebulic acid triethyl ester (Yang et al.,2020)	$C_{20}H_{22}O_{11}$	−6.7
160	hydroxycitric acid (Mekam et al.,2019)	$C_6H_8O_8$	−5.1
161	citric acid (Mekam et al.,2019)	$C_6H_8O_7$	−5.1
	Organic acids and derivatives/hydroxy acids and derivatives		
162	malic acid (Mekam et al.,2019)	$C_4H_6O_5$	−4.8
	Organic acids and derivative/organic phosphoric acid and derivative		
163	methyl bis(trimethylsilyl) phosphate (Karki et al.,2019)	$C_7H_{21}O_4PSi_2$	NA
164	1,4-digalloylquinic acid (Mahomoodally et al.,2020)	$C_{21}H_{20}O_{14}$	−7.8

(Continued on following page)

TABLE 1 | (*Continued*) Phytochemicals from *E. hirta*.

ID	Phytochemical	MF[a]	BFE[b]
165	3,5-digalloylquinic acid (Mekam et al.,2019)	$C_{21}H_{20}O_{14}$	−8.1
166	3-hydroxyoctanoic acid *O*-beta-D-glucopyranoside (Nomoto et al.,2013)	$C_{14}H_{26}O_8$	−6.1
167	hirtionoside A (Nomoto et al.,2013)	$C_{26}H_{34}O_{12}$	−8.7
168	hirtionoside B (Nomoto et al.,2013)	$C_{26}H_{34}O_{11}$	−8.8
169	hirtionoside C (Nomoto et al.,2013)	$C_{26}H_{36}O_{11}$	−8.4
	Organohalogen compound/organobromide		
170	1,5-dibromo-3-methylpentane (Rautela et al.,2020)	$C_6H_{12}Br_2$	−3.4
	Organohalogen compound/organochloride		
171	1-bromo-6-chlorohexane (Rautela et al.,2020)	$C_6H_{12}BrCl$	−3.2
	Organoheterocyclic compound/benzofuran		
172	3,6-dimethyl-5,6,7,7*a*-tetrahydro-4*H*-1-benzofuran-2-one (Rautela et al.,2020)	$C_{10}H_{14}O_2$	−5.2
	Organoheterocyclic compound/coumaran		
173	2,3-dihydrobenzofuran (Rautela et al.,2020)	C_8H_8O	−4.3
	Organoheterocyclic compound/epoxide		
174	13-oxabicyclo[10.1.0]tridecane (Karki et al.,2019)	$C_{12}H_{22}O$	−4.7
	Organoheterocyclic compounds/indoles and derivatives		
175	1,2,3,4-tetrahydrocyclopenta[*b*]indole (Rautela et al.,2020)	$C_{11}H_{11}N$	−5.4
176	tryptophan (Mekam et al.,2019)	$C_{11}H_{12}N_2O_2$	−6.1
	Organoheterocyclic compound/oxane		
177	1,3,3-trimethyl-2-oxabicyclo[2.2.2]octan-6-ol (Rautela et al.,2020)	$C_{10}H_{18}O_2$	−5.2
	Organoheterocyclic compound/oxepane		
178	3,4-epoxycyclohexylmethyl 3,4-epoxycyclohexanecarboxylate (Karki et al.,2019)	$C_{14}H_{20}O_4$	−6.2
	Organoheterocyclic compound/piperidine		
179	1-(2-piperidin-4-ylethyl)pyrrolidin-2-one (Rautela et al.,2020)	$C_{11}H_{20}N_2O$	−5.2
	Organoheterocyclic compound/pyran		
180	3,5-dihydroxy-6-methyl-2,3-dihydropyran-4-one (Sharma et al.,2014; Rautela et al.,2020)	$C_6H_8O_4$	−4.9
181	chelidonic acid (Mekam et al.,2019)	$C_7H_4O_6$	−5.8
	Organoheterocyclic compounds/pyrrolidines		
182	1-(3-methyl-3-butenyl)pyrrolidine (Rautela et al.,2020)	$C_9H_{17}N$	−4.1
183	2,2-bis(but-3-en-2-yl)pyrrolidine (Karki et al.,2019)	$C_{12}H_{21}N$	−4.4
184	1-(1-cyclohexen-1-yl)pyrrolidine (Rautela et al.,2020)	$C_{10}H_{17}N$	−4.6
	Organometallic compound/organometalloid compound		
185	diethyl-hexoxy-(3-methylbutoxy)silane (Rautela et al.,2020)	$C_{15}H_{34}O_2Si$	NA
	Organic nitrogen compound/organonitrogen compound		
186	nonanenitrile (Rautela et al.,2020)	$C_9H_{17}N$	−3.8
	Organic oxygen compounds/organooxygen compounds		
187	*cis*-5-*O*-(4-coumaroyl)-D-quinic acid (Mekam et al.,2019)	$C_{16}H_{18}O_8$	−7.5
188	trigalloylquinic acid (Mekam et al.,2019)	$C_{28}H_{24}O_{18}$	−9.0
189	cryptochlorogenic acid (Mekam et al.,2019; Mahomoodally et al.,2020)	$C_{16}H_{18}O_9$	−7.2
190	*trans*-5-*O*-(4-coumaroyl)-D-quinic acid (Mekam et al.,2019)	$C_{16}H_{18}O_8$	−7.0
191	chlorogenic acid (Mekam et al.,2019; Mahomoodally et al.,2020)	$C_{16}H_{18}O_9$	−7.2
192	*cis*-chlorogenic acid (Mekam et al.,2019)	$C_{16}H_{18}O_9$	−6.6
193	quinic acid (Mekam et al.,2019; Mahomoodally et al.,2020)	$C_7H_{12}O_6$	−5.4
194	shikimic acid (Mekam et al.,2019)	$C_7H_{10}O_5$	−5.2
195	[2,6,6-trimethyl-4-(3-methylbut-2-enyl)cyclohexen-1-yl]methanol (Olaoluwa et al.,2018)	$C_{15}H_{26}O$	−5.8
196	2-pentylcyclohexane-1,4-diol (Karki et al.,2019)	$C_{11}H_{22}O_2$	−4.7
197	quercitol(Linfang et al., 2012; Shah et al.,2019)	$C_6H_{12}O_5$	−5.4
198	(*R*)-lotaustralin (Nomoto et al.,2013)	$C_{11}H_{19}NO_6$	−6.1
199	benzyl-beta-D-glucopyranoside (Nomoto et al.,2013)	$C_{13}H_{18}O_6$	−6.7
200	rutinoside (Nomoto et al.,2013)	$C_{12}H_{22}O_{10}$	−6.8
201	(2*R*,3*S*,4*S*,5*R*,6*R*)-2-(hydroxymethyl)-6-methoxyoxane-3,4,5-triol (Rautela et al.,2020)	$C_7H_{14}O_6$	−5.3
202	ternatoside C (Mekam et al.,2019)	$C_{24}H_{23}N_3O_7$	−8.6
203	linocinnamarin (Nomoto et al.,2013)	$C_{16}H_{20}O_8$	−6.5
204	6′-*O*-galloylsalicin (Mekam et al.,2019)	$C_{20}H_{22}O_{11}$	−8.3
205	syringin (Nomoto et al.,2013)	$C_{17}H_{24}O_9$	−7.0
206	gluconic acid (Mekam et al.,2019)	$C_6H_{12}O_7$	−5.3
207	tartaric acid (Linfang et al., 2012)	$C_4H_6O_6$	−4.8
208	5-hydroxymethyl-2-furancarboxaldehyde (Sharma et al.,2014)	$C_6H_6O_3$	−4.4
209	2-hydroxy-1-(1′-pyrrolidiyl)-1-buten-3-one (Rautela et al.,2020)	$C_8H_{13}NO_2$	−4.4
210	xanthoxylin (Yang et al.,2020)	$C_{10}H_{12}O_4$	−5.3
211	megastigmatrienone A (Perumal and Mahmud, 2013)	$C_{13}H_{18}O$	−5.7
212	2-(4,4,4-trichlorobutyl)cyclohexan-1-one (Rautela et al.,2020)	$C_{10}H_{15}Cl_3O$	−4.8
213	2-butoxyethanol (Ogunlesi et al.,2009)	$C_6H_{14}O_2$	−3.7
214	2*E*,6*E*-dimethyl-2,6-octadiene-1,8-diol (Rautela et al.,2020)	$C_{10}H_{18}O_2$	−4.8

(Continued on following page)

TABLE 1 | (*Continued*) Phytochemicals from *E. hirta*.

ID	Phytochemical	MF[a]	BFE[b]
215	2-methylhexadecanol (Ogunlesi et al.,2009)	$C_{17}H_{36}O$	−4.8
	Organic salt/organic metal salt		
216	3,5-dipropyl-1,2,4,3,5-triselenadiborolane (Karki et al.,2019)	$C_6H_{14}B_2Se_3$	NA
	Phenylpropanoids and polyketide/cinnamic acids and derivative		
217	feruloyl malate (Mekam et al.,2019)	$C_{14}H_{14}O_8$	−7.0
218	*trans-para*-coumaric acid (Mekam et al.,2019)	$C_9H_8O_3$	−5.1
219	caffeic acid (Perumal et al.,2015); Mekam et al.,2019)	$C_9H_8O_4$	−5.6
220	ferulic acid (Mekam et al.,2019)	$C_{10}H_{10}O_4$	−5.7
	Phenylpropanoids and polyketides/coumarins and derivatives		
221	4-methoxyfuro[3,2-g]chromen-7-one (Rautela et al.,2020)	$C_{12}H_8O_4$	−5.8
222	isopimpinellin (Rautela et al.,2020)	$C_{13}H_{10}O_5$	−5.9
223	xanthotoxin (Rautela et al.,2020)	$C_{12}H_8O_4$	−5.9
224	esculetin (Li et al.,2015)	$C_9H_6O_4$	−6.2
225	phyllanthusiin E methyl ester (Yang et al.,2020)	$C_{14}H_{10}O_8$	−7.2
226	phyllanthusiin E (Yang et al.,2020)	$C_{13}H_8O_8$	−7.2
227	umbelliferone (Li et al.,2015)	$C_9H_6O_3$	−5.5
228	daphnoretin Li et al. (2015)	$C_{19}H_{12}O_7$	−8.4
229	scopoletin (Wu et al.,2012; Li et al.,2015; Shah et al.,2019)	$C_{10}H_8O_4$	−5.8
230	isoscopoletin (Wu et al.,2012; Li et al.,2015)	$C_{10}H_8O_4$	−5.7
231	6,7,8-trimethoxycoumarin (Sharma et al.,2014)	$C_{12}H_{12}O_5$	−5.6
232	scoparone (Wu et al.,2012; Li et al.,2015; Shah et al.,2019)	$C_{11}H_{10}O_4$	−5.7
233	citropten (Rautela et al.,2020)	$C_{11}H_{10}O_4$	−5.7
	Phenylpropanoids and polyketides/depsides and depsidones		
234	trigallic acid (Mekam et al.,2019)	$C_{21}H_{14}O_{13}$	−9.2
235	digallic acid (Mekam et al.,2019)	$C_{14}H_{10}O_9$	−8.3
	Phenylpropanoids and polyketides/diarylheptanoids		
236	tetragalloyl glucose (Mahomoodally et al.,2020)	$C_{34}H_{28}O_{22}$	−8.8
	Phenylpropanoids and polyketides/flavonoids		
237	epicatechin 3-gallate (Perumal et al.,2015; Perumal et al., 2018)	$C_{22}H_{18}O_{10}$	−8.2
238	leucocyanidol (Shah et al.,2019)	$C_{15}H_{14}O_7$	−7.2
239	epicatechin (Mekam et al.,2019)	$C_{15}H_{14}O_6$	−7.0
240	pinocembrin (Wu et al.,2012; Shah et al.,2019)	$C_{15}H_{12}O_4$	−7.2
241	chrysin (Mekam et al.,2019)	$C_{15}H_{10}O_4$	−7.3
242	luteolin (Wu et al.,2012)	$C_{15}H_{10}O_6$	−7.5
243	dimethoxyquercetin (Sheliya et al.,2015)	$C_{17}H_{14}O_9$	−7.3
244	kaempferol (Linfang et al., 2012; Wu et al.,2012; Rao et al.,2017; Ali et al.,2020)	$C_{15}H_{10}O_6$	−7.8
245	quercetin (Liu et al.,2007; Linfang et al., 2012; Wu et al.,2012; Sheliya et al.,2015; Selin-Rani et al.,2016; Bach et al.,2017; Rao et al.,2017; Suganthi and Ravi, 2018; Mekam et al.,2019; Nugroho et al.,2019; Shah et al.,2019; Ali et al.,2020; Tayone et al.,2020)	$C_{15}H_{10}O_7$	−7.5
246	isovitexin (Nomoto et al.,2013)	$C_{21}H_{20}O_{10}$	−8.0
247	kaempferol-3-*O*-glucuronide (Mekam et al.,2019)	$C_{21}H_{18}O_{12}$	−8.7
248	quercetin-3-*O*-glucuronide (Mekam et al.,2019)	$C_{21}H_{18}O_{13}$	−8.0
249	euphorbianin (Shah et al.,2019)	$C_{29}H_{32}O_{18}$	−8.2
250	myricetin-3-*O*-pentoside (Mekam et al.,2019)	$C_{20}H_{18}O_{12}$	−8.4
251	myricetin-3-*O*-hexoside (Mekam et al.,2019)	$C_{21}H_{20}O_{13}$	−7.3
252	quercetin 3-*O*-alpha-L-arabinofuranoside (Bach et al.,2020)	$C_{20}H_{18}O_{11}$	−8.5
253	quercetin-3-*O*-pentoside (Mekam et al.,2019)	$C_{20}H_{18}O_{11}$	−8.4
254	kaempferol-3-*O*-rhamnoside (Mekam et al.,2019)	$C_{21}H_{20}O_{10}$	−7.7
255	narcissin (Mekam et al.,2019)	$C_{28}H_{32}O_{16}$	−8.9
256	nicotiflorin (Mekam et al.,2019)	$C_{27}H_{30}O_{15}$	−8.7
257	afzelin (Liu et al.,2007; Nomoto et al.,2013; Shah et al.,2019; Bach et al.,2020; Mahomoodally et al.,2020)	$C_{21}H_{20}O_{10}$	−8.8
258	astragalin (Bach et al.,2020; Mahomoodally et al.,2020)	$C_{21}H_{20}O_{11}$	−8.3
259	myricetin-3-*O*-rhamnoside (Liu et al.,2007; Linfang et al., 2012; Nugroho et al.,2019; Shah et al.,2019; Bach et al.,2020; Mahomoodally et al.,2020; Tayone et al.,2020)	$C_{21}H_{20}O_{12}$	−9.0
260	isorhamnetin (Wu et al.,2012; Shah et al.,2019)	$C_{21}H_{20}O_{12}$	−7.3
261	hyperoside (Mekam et al.,2019)	$C_{21}H_{20}O_{12}$	−8.5
262	rutin (Linfang et al., 2012; Bach et al.,2017; Rao et al.,2017; Suganthi and Ravi, 2018; Mekam et al.,2019; Ali et al.,2020; Mahomoodally et al.,2020)	$C_{27}H_{30}O_{16}$	−8.8
263	isoquercitrin (Mekam et al.,2019; Mahomoodally et al.,2020)	$C_{21}H_{20}O_{12}$	−8.0
264	quercetin-3-*O*-rhamnoside (Gopi et al.,2016; Mekam et al.,2019; Mahomoodally et al.,2020)	$C_{21}H_{20}O_{11}$	−9.0
265	luteolin-7-*O*-beta-D-glucopyranoside (Bach et al.,2020)	$C_{21}H_{20}O_{11}$	−7.9
266	cosmosiin (Mahomoodally et al.,2020)	$C_{21}H_{20}O_{10}$	−7.8
267	scutellarein 6-glucoside (Mekam et al.,2019)	$C_{21}H_{20}O_{11}$	−7.8
268	hymenoxin (Bach et al.,2020)	$C_{19}H_{18}O_8$	−7.0

(Continued on following page)

TABLE 1 | (*Continued*) Phytochemicals from *E. hirta*.

ID	Phytochemical	MF[a]	BFE[b]
	Phenylpropanoids and polyketides/isocoumarins and derivatives		
269	brevifolin (Yang et al.,2020)	$C_{12}H_8O_6$	−7.2
270	ethyl brevifolin carboxylate (Yang et al.,2020)	$C_{15}H_{12}O_8$	−7.0
271	brevifolin carboxylic acid (Mahomoodally et al.,2020; Yang et al.,2020)	$C_{13}H_8O_8$	−7.2
272	methyl brevifolin carboxylate (Yang et al.,2020)	$C_{14}H_{10}O_8$	−6.4
	Phenylpropanoids and polyketides/tannins		
273	tannic acid (Yang et al.,2020)	$C_{76}H_{52}O_{46}$	−7.1
274	ellagitannin (Yang et al.,2020)	$C_{44}H_{32}O_{27}$	−8.5
275	ellagic acid (Linfang et al., 2012; Mekam et al.,2019; Mahomoodally et al.,2020)	$C_{14}H_6O_8$	−7.3
276	pedunculagin II (Mekam et al.,2019)	$C_{34}H_{26}O_{22}$	−8.9
277	pedunculagin (Mekam et al.,2019)	$C_{34}H_{24}O_{22}$	−8.0
278	corilagin (Mekam et al.,2019; Mahomoodally et al.,2020)	$C_{27}H_{22}O_{18}$	−8.7
279	penta-*O*-galloylglucose (Mekam et al.,2019; Mahomoodally et al.,2020)	$C_{41}H_{32}O_{26}$	−8.0
	Phenylpropanoids and polyketides		
280	(*R*)-euphorhirtin H (Yang et al.,2020)	$C_{16}H_{12}O_{10}$	−7.7
281	(*R*)-euphorhirtin I (Yang et al.,2020)	$C_{15}H_{10}O_{10}$	−7.5
282	(*R*)-euphorhirtin J (Yang et al.,2020)	$C_{17}H_{14}O_{10}$	−7.6
283	(*R*)-euphorhirtin K (Yang et al.,2020)	$C_{18}H_{16}O_{10}$	−7.5
284	(*R*)-euphorhirtin L (Yang et al.,2020)	$C_{18}H_{16}O_{10}$	−6.4
285	(*R*)-euphorhirtin M (Yang et al.,2020)	$C_{17}H_{16}O_9$	−6.4
286	(*S*)-euphorhirtin H (Yang et al.,2020)	$C_{16}H_{12}O_{10}$	−7.0
287	(*S*)-euphorhirtin I (Yang et al.,2020)	$C_{15}H_{10}O_{10}$	−7.0
288	(*S*)-euphorhirtin J (Yang et al.,2020)	$C_{17}H_{14}O_{10}$	−6.9
289	(*S*)-euphorhirtin K (Yang et al.,2020)	$C_{18}H_{16}O_{10}$	−6.6
290	(*S*)-euphorhirtin L (Yang et al.,2020)	$C_{18}H_{16}O_{10}$	−7.2
291	(*S*)-euphorhirtin M (Yang et al.,2020)	$C_{17}H_{16}O_9$	−6.6
292	5-*O*-feruloylquinic acid (Mekam et al.,2019)	$C_{17}H_{20}O_8$	−7.2
293	chebulic acid-14,15-diethyl ester (Yang et al.,2020)	$C_{18}H_{20}O_{11}$	−6.5
294	euphorhirtin E (Yang et al.,2020)	$C_{18}H_{18}O_{11}$	−6.7
295	euphorhirtin F (Yang et al.,2020)	$C_{18}H_{20}O_{11}$	−6.1
296	euphorhirtin G (Yang et al.,2020)	$C_{15}H_{12}O_8$	−6.9
297	euphorhirtin N (Yang et al.,2020)	$C_{20}H_{21}NO_9$	−7.5
298	feruloylconiferin (Mekam et al.,2019)	$C_{26}H_{28}O_{12}$	−8.5
	Negative controls		
N1	anthracene	$C_{14}H_{10}$	−5.8
N2	naphthalene	$C_{10}H_8$	−4.8
N3	glycerol	$C_3H_8O_3$	−3.9
N4	decane	$C_{10}H_{22}$	−3.7
N5	hexanol	$C_6H_{12}O$	−3.5
N6	benzene	C_6H_6	−3.3
N7	cyclohexane	C_6H_{12}	−3.3
N8	hexane	C_6H_{14}	−3.1
N9	ethanol	C_2H_6	−2.4
N10	water	H_2O	−1.8
	Positive controls		
P1	efonidipine	$C_{34}H_{38}N_{3O7}P$	−8.2
P2	bedaquiline	$C_{32}H_{31}BrN_2O_2$	−8.0
P3	tideglusib	$C_{19}H_{14}N_2O_2S$	−7.9
P4	manidipine	$C_{35}H_{38}N_4O_6$	−7.6
P5	N3	$C_{35}H_{48}N_{6O8}$	−7.5
P6	lercanidipine	$C_{36}H_{41}N_3O_6$	−7.4
P7	boceprevir	$C_{27}H_{45}N_5O_5$	−7.2
P8	shikonin	$C_{16}H_{16}O_5$	−6.8
P9	ebselen	$C_{13}H_9NOSe$	−6.6
P10	carmofur	$C_{11}H_{16}FN_3O_3$	−6.0

*Notes: a, molecular formula; b, computed BFE in kcal/mol using AutoDock Vina implemented in PyRx0.8. Phytochemicals with NA, indicated for their BFE, contain atoms that are not well parameterized for molecular docking using PyRx0.8.Benzenoids contain the benzene ring; hydrocarbons are composed of H and C atoms only; lignans contain dimeric phenylpropanoids; lipids contain isoprene moiety (terpene or terpenoids), fatty acyls, and derivatives; OADs contain the acyl group; OOCs contain oxygen atoms (e.g., alcohols and esters); OHCC, heterocyclic ring; PPPK, Ph-C3- and alternating-(C = O)-CH_2-. * Miscellaneous groups are composed of the least abundant phytochemicals.*

components of *E. hirta* were identified from verified sources. This is by far the most comprehensive data gathering for *E. hirta* phytochemicals. The phytochemicals gathered fall into 13 ClassyFire Superclass levels. Majority are lipids and lipid-like molecules (Lipids) (108, 36.2%); phenylpropanoids and polyketides (PPPKs) (82, 27.5%); organic oxygen compounds

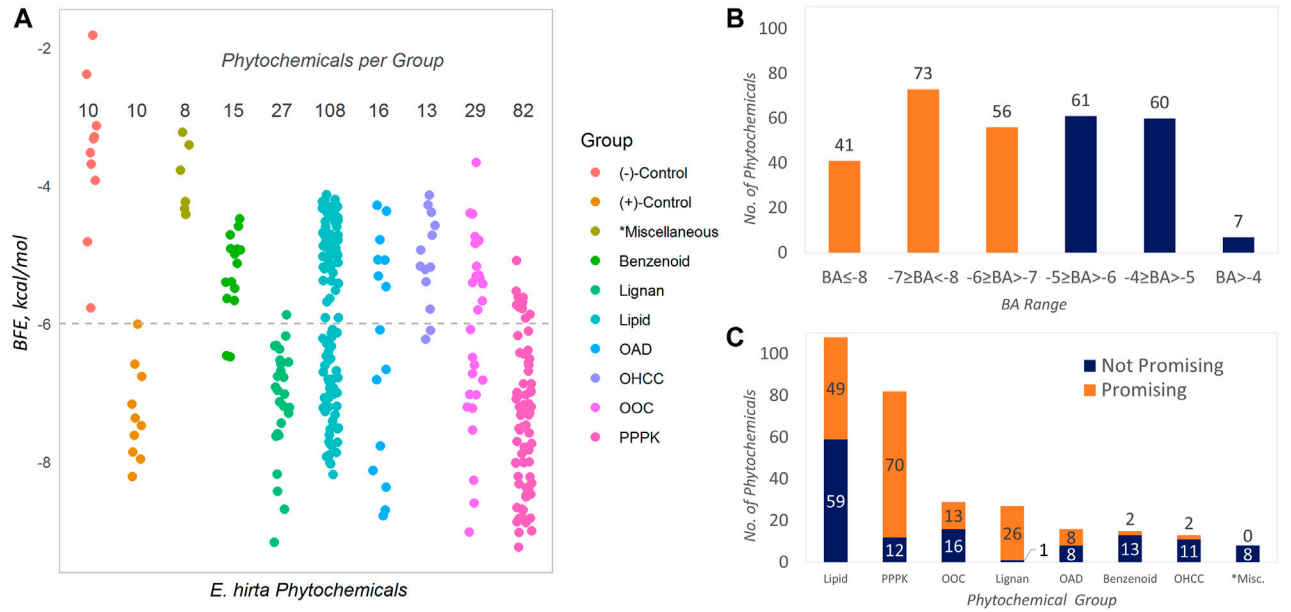

FIGURE 1 | Binding properties of the phytochemicals from *E. hirta* against SARS-CoV-2 main protease. Benzenoids contain the benzene ring; hydrocarbons are composed of H and C atoms only; lignans contain dimeric phenylpropanoids; lipids contain isoprene moiety (terpene or terpenoids), fatty acyls, and derivatives; OADs contain the acyl group; OOCs contain oxygen atoms (e.g., alcohols and esters); OHCC, heterocyclic ring; PPPK, Ph-C3- and alternating—(C=O)-CH_2-. *Miscellaneous groups are composed of the least abundant phytochemicals.

(OOCs) (29, 9.7%); lignan, neolignans, and related compounds (Lignans) (27, 9.1%); organic acids and derivatives (OADs) (16, 5.4%); benzenoids (15, 5.0%); and organoheterocyclic compounds (OHCCs) (13, 4.4%), comprising a total of 97.0%. The rest (*Miscellaneous) of the phytochemicals are hydrocarbons, organic 1,3-dipolar compounds, organic nitrogen, organohalogens, and organic salt.

3.2 Virtual Screening Through Automated Molecular Docking

The data obtained in **Table 1** are graphically presented in **Figure 1**. The BFE values of the phytochemicals are described in **1A**, and these are compared to the control compounds (positive and negative). It can be observed that the positive controls obtained more highly negative BFE values (thermodynamically stable receptor–ligand interaction) against SARS-CoV-2 Mpro than the negative controls (see entries in **Table 1**). The least negative in the group is that of carmofur with −6.0 kcal/mol computed BFE based on the AutoDock Vina docking algorithm. This value (−6.0 kcal/mol) was taken as the threshold for assigning promising inhibitors considering the fact that carmofur and the rest of the positive control compounds are actual *in vitro* inhibitors against SARS-CoV-2 Mpro. Phytochemicals having BFE values of ≤−6.0 kcal/mol qualify as promising inhibitors. In **Figure 1A**, these phytochemicals are represented by the points on and below the dashed horizontal line. Over this line are the non-promising inhibitors and the negative controls with less satisfactory BFE values. Overall, 170 (57.0%) of the phytochemicals found in *E. hirta* were identified as promising inhibitors against SARS-CoV-2 Mpro from a total of 298 phytochemicals.

The distribution of the BFEs is shown in **Figure 1B** and that of the promising inhibitors is highlighted as orange bars. The BFE range with the most abundant phytochemicals is $-7 \geq \text{BFE} < -8$ with 73 (24.5%) promising inhibitors. It can be seen in both **Figure 1A** and **Figure 1C** that the two most abundant groups are lipids (108, 36.2%) and PPPKs (82, 27.5%), collectively comprising 63.7% of the total. Interestingly, PPPKs have the most number of promising phytochemicals per group. There are 70 out of 82 (85.4%) PPPKs that are promising inhibitors. This value is 23.5% of the total number of *E. hirta* phytochemicals. This behavior by the PPPKs has been previously noted (Cayona and Creencia, 2021a, Cayona and Creencia, 2022). The relative numbers of promising and non-promising inhibitors with respect to chemical grouping are given in **Figure 1C**.

3.3 Antiviral Phytochemicals From *E. hirta*

Virtual screening revealed that *E. hirta* is an abundant source of promising inhibitors of SARS-CoV-2 Mpro. The list of promising inhibitors includes notable compounds with interesting biological and pharmacological properties. At least 12 of the promising inhibitors were established *in vitro* or *in vivo* antiviral compounds against various viruses. These are kaempferol (A), luteolin (B), quercetin (C), isoquercitrin (D), hyperoside (E), rutin (F), myricetin-3-*O*-rhamnoside (G), daphnoretin (H), digallic acid (I), epicatechin-3-gallate (J), trigallic acid (K), and corilagin (L). The chemical structures of the aforementioned compounds and their overlain conformations on the active site of SARS-CoV-2 Mpro represented by an H-bonding surface are shown in

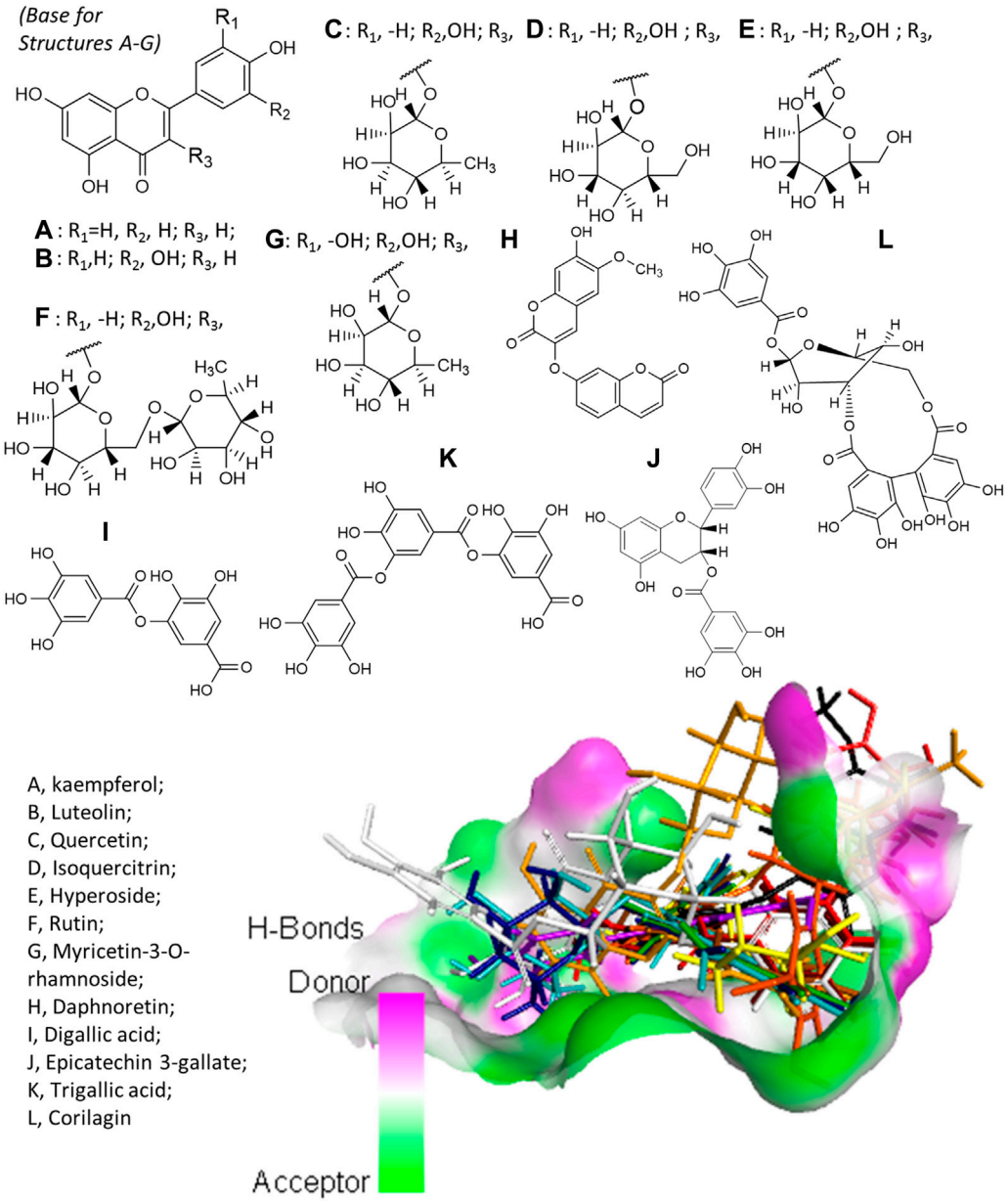

FIGURE 2 | Structures of the antiviral compounds found in *E. hirta* and overlain stick representation of the ligands in complex with SARS-CoV-2 Mpro. **(A)** Brown; **(B)** purple; **(C)** mint green; **(D)** cyan; **(E)** blue; **(F)** gold; **(G)** yellow; **(H)** black; **(I)** maroon; **(J)** orange; **(K)** red; and **(L)** gray.

Figure 2. A–G all have a common molecular skeleton, of which A is the only one without an attached sugar moiety. The skeleton of H is an isomer of A–G skeleton, and I–L are gallic acid derivatives.

The viruses susceptible to compounds A–L are listed in **Table 2** along with relevant details obtained from virtual screening (i.e., BFEs and interacting AAs). The susceptible viruses include herpes simplex virus (HSV), hepatitis, enterovirus, human immunodeficiency virus (HIV), and influenza. Interestingly, specific antivirals are effective against viruses that affect the respiratory tract, such as CoVs and respiratory syncytial viruses (RSVs). This property is clearly relevant when considering chemical therapy against respiratory tract-related diseases like COVID-19. Kaempferol is active against CoVs (Schwarz et al., 2014), and luteolin (Wang S. et al., 2020) and daphnoretin (Wang S. et al., 2020) are active against RSVs.

The interacting AAs are obtained from the most stable molecular docking conformation. These AAs are located at least 3.5 Å from the nearest atom of the docked ligands. It can be observed in **Table 2** that H41 and/or C145 (in boldface) catalytic dyad residues in the active site of SARS-CoV-2 Mpro can interact with the promising inhibitors (identified using DSV

TABLE 2 | *In vitro* antiviral phytochemicals rediscovered from the medicinal plants used in this study.

***	Phytochemical	BFE[a]	Interacting AAs[b]	Susceptible viruses[c]
A	Kaempferol	−7.8	**H41**, M49, L141, **C145**, H163, E166, M165, R188	HSV-1 (Zhu et al.,2018); **CoV** (Schwarz et al.,2014)
B	Luteolin	−7.5	N142, **C145**, M165, R188, T190	**RSV** (Wang S et al.,2020); HSV (Béládi et al.,1977; Fan et al.,2016; Xu et al.,2000)
C	Quercetin	−7.5	M49, L141, **C145**, M165, E166, Q189	HSVs (Gaudry et al.,2018; Kim et al.,2020; Xu et al.,2000)
D	Isoquercitrin	−8.0	**H41**, M49, L141, **C145**, M165, E166, P168, D187, Q189, T190	HSV (Gaudry et al.,2018; Kim et al.,2020; Xu et al.,2000)
E	Hyperoside	−8.5	M49, L141, **C145**, M165, E166, R188, Q189, T190, Q192	Hepa B (Wu et al.,2007)
F	Rutin	−8.8	T26, L141, N142, G143, **C145**, H163, M165, E166, R188, Q189, T190	HSVs (Béládi et al.,1977); HIV-1 (Xu et al.,2000); enterovirus (Lin et al.,2012)
G	Myricetin-3-*O*-rhamnoside	−9.0	M49, L141, N142, S144, **C145**, E166	Hepa B (Parvez et al.,2020); influenza A (Motlhatlego et al.,2021); HIV-1 (Ortega et al.,2017)
H	Daphnoretin	−8.4	**H41,** G143, **C145,** M165	**RSV** (Ho et al.,2010; Hu et al.,2000)
I	Digallic acid	−8.3	L141, G143, S144, **C145**, H163, H164, M165, E166, R188	HIV (Nakane et al.,1990)
J	Epicatechin 3-gallate	−8.2	**H41**, F140, L141, N142, **C145**, M165, E166, H172	HSV-2 (Alvarez et al.,2012)
K	Trigallic acid	−9.2	T26, L141, G143, S144, **C145**, M165, E166, H163, Q189	HIV (Nakane et al.,1990)
***L	Corilagin	−8.7	L141, N142, G143, S144, **C145**, H163, E166, P168, T190, Q192	HSV-1 (Guo et al.,2015); Hepa C (Reddy et al.,2018)

Notes: a, computed binding affinity towards SARS-CoV-2, Mpro in kcal/mol; b, interacting AA residues of the most stable conformation of the docked ligands; c, based on reported in vitro *antiviral activity (HSV, herpes simplex virus; RSV, respiratory syncytial virus; HIV, human immunodeficiency virus; Hepa, hepatitis).*

2020); however, molecular dynamics (MD) simulations are necessary to assess the stability of the receptor–ligand complex that can be formed. As stated previously, MD simulations are not covered in the scope of the present study and are reserved for future analyses. Nevertheless, the identification of these dyad residues in close proximity to the docked ligands provides a rationale for further studies. **Figure 3** shows how the most stable docked conformations of kaempferol (one of the promising inhibitors) and N3 (known inhibitor) fit into the active site of SARS-CoV-2 Mpro. The AAs that are in close proximity to the ligands are also shown.

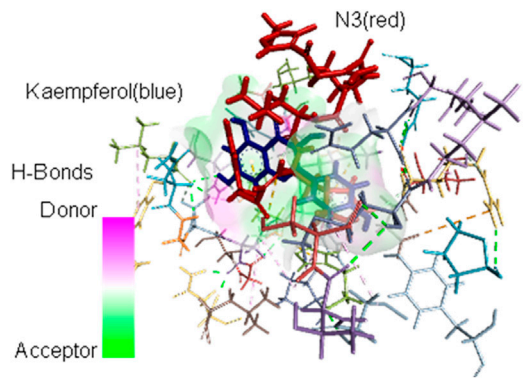

FIGURE 3 | Most stable conformations of the docked kaempferol (blue) and the inhibitor N3 (red) into the active site of SARS-CoV-2 Mpro showing the AA residues near the ligands.

4 DISCUSSION

This study provides the most comprehensive phytochemical gathering for *E. hirta* at present. It is argued in this the study that organized phytochemical composition will generate new information and enable meaningful analyses that may aid in understanding phytochemistry and plant metabolism. It was quite unexpected to discover an abundant cocktail of potential SARS-CoV-2 Mpro inhibitors from a single plant species. Clearly, lipids and PPPKs are among the most diverse groups of phytochemicals in *E. hirta*. These groups are also observed to be significantly more abundant in quantity than other phytochemical groups in *E. hirta* extracts (Sharma et al., 2014; Rao et al., 2017).

The molecular surface representation of the receptor reveals abundant hydrogen donor (purple) and acceptor (green) sites. This partly explains the observation that the ligands that can effectively establish H-bonding generally possess more negative BFEs than those that do not. Careful examination of the individual structures of the phytochemicals tested revealed that the capacity for H-bonding signifies direct correlation to favorable BFE. The ligands represented by the points below the dashed horizontal line in **Figure 1A** can H-bond more effectively and have more negative BFE towards SARS-CoV-2 Mpro than the ones above the line. Hydrocarbons (*Miscellaneous group), benzenoids, and OHCCs are obviously represented in the latter because they cannot (or can poorly) establish H-bonding with the receptor.

The molecular docking behavior of most PPPKs is interesting and deserves further investigation. Their docked conformations like the one presented in **Figure 2** indicate the molecular skeleton that deeply buried and extended through the active site cavity of SARS-CoV-2 Mpro. The phenylpropanoids and their structurally related groups, the lignans, may feature pharmacophoric moieties.

Available preclinical information conclusively reveals that *E. hirta* possesses antiviral properties (Perera et al., 2018). In this study, some of these antiviral phytochemicals with established antiviral properties against various viruses, including those that affect the respiratory tract, were rediscovered through the PM-VS strategy. These properties are relevant in the effort to address a respiratory disease like COVID-19. More importantly, the strategy allowed the identification of many other promising inhibitors of SARS-CoV-2 Mpro despite its simplicity. Further studies are definitely necessary, but preliminary results gathered on the demonstration of the proof-of-principle for PM-VS provide a basis for exhaustive *in silico* investigations and future *in vitro* experiments. PM-VS can be efficiently implemented in the preliminary stages of drug discovery and development with minimal computational cost. Moving forward, other drug targets, not only COVID-19 drug targets, can also be investigated with PM-VS using different medicinal plants.

5 CONCLUSION

A method described as phytochemical mining allowed the systematic collection and organization of phytochemical components from *E. hirta*. A total of 298 *E. hirta* phytochemicals collected from the literature represent the most comprehensive phytochemical data collection for the plant. Virtual screening through molecular docking of the phytochemicals revealed an abundant cocktail of 170 promising inhibitors against SARS-CoV-2 Mpro. Twelve of the promising inhibitors are also prominent natural products with reported antiviral property against diverse viruses including respiratory CoV and RSVs. Finally, PM-VS was successfully implemented in this study, and the preliminary results obtained so far suggest further investigations.

DATA AVAILABILITY STATEMENT

The raw data supporting the conclusion of this article will be made available by the authors, without undue reservation.

AUTHOR CONTRIBUTIONS

The authors (RC and EC) contributed equally to the conceptualization, data gathering, analysis, and manuscript preparation.

ACKNOWLEDGMENTS

The authors acknowledge the Drug Design and Development Related Research Lab (DDDRRL) of the Premier Research Institute of Science and Mathematics (PRISM), MSU-IIT, for supporting this study. RC thanks DOST-SEI for the scholarship grant under ASTHRDP-NSC.

SUPPLEMENTARY MATERIAL

The Supplementary Material for this article can be found online at: https://www.frontiersin.org/articles/10.3389/fmolb.2021.801401/full#supplementary-material

REFERENCES

Ali, M. Z., Mehmood, M. H., Saleem, M., and Gilani, A.-H. (2020). The Use of Euphorbia Hirta L. (Euphorbiaceae) in Diarrhea and Constipation Involves Calcium Antagonism and Cholinergic Mechanisms. *BMC Complement. Med. Ther.* 20 (1), 14. doi:10.1186/s12906-019-2793-0

Álvarez, Á. L., Dalton, K. P., Nicieza, I., Diñeiro, Y., Picinelli, A., Melón, S., et al. (2012). Bioactivity-Guided Fractionation of Phyllanthus Orbicularis and Identification of the Principal Anti HSV-2 Compounds. *Phytother. Res.* 26 (10), 1513–1520. doi:10.1002/ptr.4608

Amos Samkumar, R., Premnath, D., and David Paul Raj, R. S. (2019). Strategy for Early Callus Induction and Identification of Anti-snake Venom Triterpenoids from Plant Extracts and Suspension Culture of Euphorbia Hirta L. *3 Biotech.* 9 (7), 266. doi:10.1007/s13205-019-1790-9

Bach, L. T., Dung, L. T., Quetin-Leclereq, J., Kestermont, P., Scippo, M.-L., Phuong, T. N., et al. (2017). The Flavonoid Isolation and Antioxidant Activity of *Euphorbia Hirta* L. Extracts. *Vietnam J. Chem.* 55 (5E34), 568–573. Retrieved from: https://aquabioactive.ctu.edu.vn/images/upload/publications/bai-bao-chi-bach.pdf

Bach, L. T., Hue, B. T. B., Tram, N. T. T., Thu, D. N. A., and Dung, L. T. (2020). Chemical Constituents from N-Hexane and Ethyl Acetate Extracts of Euphorbia Hirta L. Grown in Vietnam. *IOP Conf. Ser. Mater. Sci. Eng.* 736, 022083. doi:10.1088/1757-899X/736/2/022083

Béládi, I., Pusztai, R., Mucsi, I., Bakay, M., and Gábor, M. (1977). Activity of Some Flavonoids against Viruses. *Ann. NY Acad. Sci.* 284 (1 Third Confere), 358–364. doi:10.1111/j.1749-6632.1977.tb21971.x

Cayona, R., and Creencia, E. (2021a). Discovery of a "Cocktail" of Potential SARS-COV-2 Main Protease Inhibitors through Virtual Screening of Known Chemical Components of Vitex Negundo L. ("Lagundi"). *Med. Chem.* 18 (3), 364381. doi:10.2174/1573406417666210618132003

Cayona, R., and Creencia, E. (2021b). Phytochemical Mining Of SARS-COV-2 Main Protease Inhibitors From the Philippine Medicinal Plants*: Vitex Negundo, Blumea Balsamifera, Euphorbia Hirta, Catharanthus Roseus, Mentha Cordifolia, Ehretia Microphylla, Combretum Indicum, Lagerstroemia Speciosa, Peperomia Pellucida, and Senna alata [Dissertation]*. Iligan City: Mindanao State University-Iligan Institute of Technology.

Cayona, R., and Creencia, E. (2022). Phytochemical Mining of Potential SARS-CoV-2 Main Protease Inhibitors from *Blumea Balsamifera* (L.) DC. *Philippine J. Sci.* 151 (1), 235–261. Retrieved from: https://philjournalsci.dost.gov.ph/111-vol-151-no-1-february-2022/1555-phytochemical-mining-of-potential-sars-cov-2-main-protease-inhibitors-from-blumea-balsamifera-l-dc

Chi, S.-M., Wang, Y., Zhao, Y., Pu, J.-X., Du, X., Liu, J.-P., et al. (2012). A New Cyclopentanone Derivative from Euphorbia Hirta. *Chem. Nat. Compd.* 48 (4), 577–579. doi:10.1007/s10600-012-0315-0

Dallakyan, S., and Olson, A. J. (2015). "Small-Molecule Library Screening by Docking with PyRx," in *Chemical Biology: Methods and Protocols*. Editors J. E. Hempel, C. H. Williams, and C. C. Hong (Springer), 243–250. doi:10.1007/978-1-4939-2269-7_19

Dayrit, F. M., Jr, A. M. G., and Gloriani, N. G. (2021). Philippine Medicinal Plants with Potential Immunomodulatory and Anti-SARS-CoV-2 Activities. *Philippine J. Sci.* 150 (5), 17. Retrieved from: https://philjournalsci.dost.gov.ph/108-vol-150-no-5-october-2021/1467-philippine-medicinal-plants-with-potential-immunomodulatory-and-anti-sars-cov-2-activities

Di Micco, S., Musella, S., Scala, M. C., Sala, M., Campiglia, P., Bifulco, G., et al. (2021). *In Silico* Analysis Revealed Potential Anti-SARS-CoV-2 Main Protease Activity by the Zonulin Inhibitor Larazotide Acetate. *Front. Chem.* 8, 628609. doi:10.3389/fchem.2020.628609

Djoumbou Feunang, Y., Eisner, R., Knox, C., Chepelev, L., Hastings, J., Owen, G., et al. (2016). ClassyFire: Automated Chemical Classification with a Comprehensive, Computable Taxonomy. *J. Cheminform.* 8 (1), 61. doi:10.1186/s13321-016-0174-y

Ekpo, O. E., and Pretorius, E. (2007). Asthma, Euphorbia Hirta and its Anti-Inflammatory Properties. *South Afr. J. Sci.* 103 (5), 201–203. Retrieved from: https://www.researchgate.net/publication/286838495_Asthma_Euphorbia_hirta_and_its_anti-inflammatory_properties

Fan, W., Qian, S., Qian, P., and Li, X. (2016). Antiviral Activity of Luteolin against Japanese Encephalitis Virus. *Virus. Res.* 220, 112–116. doi:10.1016/j.virusres.2016.04.021

Gaudry, A., Bos, S., Viranaicken, W., Roche, M., Krejbich-Trotot, P., Gadea, G., et al. (2018). The Flavonoid Isoquercitrin Precludes Initiation of Zika Virus Infection in Human Cells. *Int. J. Mol. Sci.* 19 (4), 1093. doi:10.3390/ijms19041093

Ghahremanpour, M. M., Tirado-Rives, J., Deshmukh, M., Ippolito, J. A., Zhang, C.-H., Cabeza de Vaca, I., et al. (2020). Identification of 14 Known Drugs as Inhibitors of the Main Protease of SARS-CoV-2. *ACS Med. Chem. Lett.* 11 (12), 2526–2533. doi:10.1021/acsmedchemlett.0c00521

Gopi, K., Anbarasu, K., Renu, K., Jayanthi, S., Vishwanath, B. S., and Jayaraman, G. (2016). Quercetin-3-O-rhamnoside from Euphorbia Hirta Protects Against Snake Venom Induced Toxicity. *Biochim. Biophys. Acta (Bba) - Gen. Subjects.* 1860 (7), 1528–1540. doi:10.1016/j.bbagen.2016.03.031

Guo, Y.-J., Luo, T., Wu, F., Liu, H., Li, H.-R., Mei, Y.-W., et al. (2015). Corilagin Protects Against HSV1 Encephalitis through Inhibiting the TLR2 Signaling Pathways *In Vivo* and *In Vitro*. *Mol. Neurobiol.* 52 (3), 1547–1560. doi:10.1007/s12035-014-8947-7

Guzman, G., Dacanay, A., Andaya, B., and Alejandro, G. (2016). Ethnopharmacological Studies on the Uses of Euphorbia Hirta in the Treatment of Dengue in Selected Indigenous Communities in Pangasinan (Philippines). *J. Intercult Ethnopharmacol.* 5 (3), 239–243. doi:10.5455/jice.20160330124637

Hakmi, M., Bouricha, E. M., Kandoussi, I., Harti, J. E., and Ibrahimi, A. (2020). Repurposing of Known Anti-Virals as Potential Inhibitors for SARS-CoV-2 Main Protease Using Molecular Docking Analysis. *Bioinformation.* 16 (4), 301. doi:10.6026/97320630016301

Ho, W.-S., Xue, J.-Y., Sun, S. S. M., Ooi, V. E. C., and Li, Y.-L. (2010). Antiviral Activity of Daphnoretin Isolated from Wikstroemia Indica. *Phytother. Res.* 24 (5), 657–661. doi:10.1002/ptr.2935

Hu, K., Kobayashi, H., Dong, A., Iwasaki, S., and Yao, X. (2000). Antifungal, Antimitotic and Anti-HIV-1 Agents from the Roots of Wikstroemia Indica. *Planta Med.* 66 (6), 564–567. doi:10.1055/s-2000-8601

Jin, Z., Du, X., Xu, Y., Deng, Y., Liu, M., Zhao, Y., et al. (2020). Structure of Mpro from SARS-CoV-2 and Discovery of its Inhibitors. *Nature.* 582 (7811), 289–293. doi:10.1038/s41586-020-2223-y

Karki, S., Shrestha, K., Gautam, R., and Narayan, R. (2019). Phytochemical Screening, FT-IR and GC-MS Analysis of *Euphorbia Hirta*. *J. Pharmacognosy Phytochemistry.* 9 (1), 1883–1889. Retrieved from: https://www.researchgate.net/publication/349124683_Phytochemical_screening_FT-IR_and_GC-MS_analysis_of_Euphorbia_hirta

Khan, A., Ali, S. S., Khan, M. T., Saleem, S., Ali, A., Suleman, M., et al. (2020). Combined Drug Repurposing and Virtual Screening Strategies with Molecular Dynamics Simulation Identified Potent Inhibitors for SARS-CoV-2 Main Protease (3CLpro). *J. Biomol. Struct. Dyn.* 39 (0), 4659–4670. doi:10.1080/07391102.2020.1779128

Kim, C. H., Kim, J.-E., and Song, Y.-J. (2020). Antiviral Activities of Quercetin and Isoquercitrin Against Human Herpesviruses. *Molecules.* 25 (10), 2379. doi:10.3390/molecules25102379

Li, E.-T., Liu, K.-H., Zang, M.-H., Zhang, X.-L., Jiang, H.-Q., Zhou, H.-L., et al. (2015). Chemical Constituents from Euphorbia Hirta. *Biochem. Syst. Ecol.* 62, 204–207. doi:10.1016/j.bse.2015.09.007

Lin, Y.-J., Chang, Y.-C., Hsiao, N.-W., Hsieh, J.-L., Wang, C.-Y., Kung, S.-H., et al. (2012). Fisetin and Rutin as 3C Protease Inhibitors of Enterovirus A71. *J. Virol. Methods.* 182 (1), 93–98. doi:10.1016/j.jviromet.2012.03.020

Linfang, H., Shilin, C., and Meihua, Y. (2012). Euphorbia Hirta (Feiyangcao): A Review on its Ethnopharmacology, Phytochemistry and Pharmacology. *J. Med. Plants Res.* 6 (39), 5176–5185. doi:10.5897/JMPR12.206

Liu, Y., Murakami, N., Ji, H., Abreu, P., and Zhang, S. (2007). Antimalarial Flavonol Glycosides fromEuphorbia Hirta. *Pharm. Biol.* 45 (4), 278–281. doi:10.1080/13880200701214748

Luci-Atienza, C. (2021a). 68 COVID-19 Patients Already Recruited to Participate in PH's Tawa-Tawa Clinical Trial. Manila Bulletin. Available at: https://mb.com.ph/2021/07/02/68-covid-19-patients-already-recruited-to-participate-in-phs-tawa-tawa-clinical-trial/.

Luci-Atienza, C. (2021b). Recruitment of Volunteers for PH Clinical Trial for Tawa-Tawa as COVID-19 Treatment Still Ongoing—DOST. Manila Bulletin. Available at: https://mb.com.ph/2021/08/27/recruitment-of-volunteers-for-ph-clinical-trial-for-tawa-tawa-as-covid-19-treatment-still-ongoing-dost/.

Ma, C., Hu, Y., Townsend, J. A., Lagarias, P. I., Marty, M. T., Kolocouris, A., et al. (2020). Ebselen, Disulfiram, Carmofur, PX-12, Tideglusib, and Shikonin Are Nonspecific Promiscuous SARS-CoV-2 Main Protease Inhibitors. *ACS Pharmacol. Transl. Sci.* 3 (6), 1265–1277. doi:10.1021/acsptsci.0c00130

Mahomoodally, M. F., Dall'Acqua, S., Sinan, K. I., Sut, S., Ferrarese, I., Etienne, O. K., et al. (2020). Phenolic Compounds Analysis of Three Euphorbia Species by LC-DAD-MSn and Their Biological Properties. *J. Pharm. Biomed. Anal.* 189, 113477. doi:10.1016/j.jpba.2020.113477

Mallavadhani, U. V., and Narasimhan, K. (2009). Two Novel Butanol Rhamnosides from an Indian Traditional Herb,Euphorbia Hirta. *Nat. Product. Res.* 23 (7), 644–651. doi:10.1080/14786410802214009

Martínez-Vázquez, M., Apan, T. O. R., Lazcano, M. E., and Bye, R. (1999). Anti-inflammatory Active Compounds from the N-Hexane Extract of Euphorbia Hirta. *J. Mexican Chem. Soc.* 43 (3,4), 103–105. Retrieved from: https://www.redalyc.org/pdf/475/47543410.pdf

Mekam, P. N., Martini, S., Nguefack, J., Tagliazucchi, D., and Stefani, E. (2019). Phenolic Compounds Profile of Water and Ethanol Extracts of Euphorbia Hirta L. Leaves Showing Antioxidant and Antifungal Properties. *South Afr. J. Bot.* 127, 319–332. doi:10.1016/j.sajb.2019.11.001

Menéndez, C. A., Byléhn, F., Perez-Lemus, G. R., Alvarado, W., and de Pablo, J. J. (2020). Molecular Characterization of Ebselen Binding Activity to SARS-CoV-2 Main Protease. *Sci. Adv.* 6 (37), eabd0345. doi:10.1126/sciadv.abd0345

Mirza, M. U., and Froeyen, M. (2020). Structural Elucidation of SARS-CoV-2 Vital Proteins: Computational Methods Reveal Potential Drug Candidates Against Main Protease, Nsp12 Polymerase and Nsp13 Helicase. *J. Pharm. Anal.* 10 (4), 320–328. doi:10.1016/j.jpha.2020.04.008

Moher, D., Liberati, A., Tetzlaff, J., Altman, D. G., and Group, T. P. (2009). Preferred Reporting Items for Systematic Reviews and Meta-Analyses: The PRISMA Statement. *Plos Med.* 6 (7), e1000097. doi:10.1371/journal.pmed.1000097

Morris, G. M., Huey, R., Lindstrom, W., Sanner, M. F., Belew, R. K., Goodsell, D. S., et al. (2009). AutoDock4 and AutoDockTools4: Automated Docking with Selective Receptor Flexibility. *J. Comput. Chem.* 30 (16), 2785–2791. doi:10.1002/jcc.21256

Motlhatlego, K. E., Mehrbod, P., Fotouhi, F., Abdalla, M. A., Eloff, J. N., and McGaw, L. J. (2021). Anti-influenza A Virus Activity of Two Newtonia Species and the Isolated Compound Myricetin-3-O-Rhamnoside. *BMC Complement. Med. Ther.* 21 (1), 92. doi:10.1186/s12906-021-03250-0

Nakane, H., Fukushima, M., and Ono, K. (1990). Differential Inhibition of Reverse Transcriptase and Various DNA Polymerases by Digallic Acid and its Derivatives. *J. Nat. Prod.* 53 (5), 1234–1240. doi:10.1021/np50071a015

Nomoto, Y., Sugimoto, S., Matsunami, K., and Otsuka, H. (2013). Hirtionosides A-C, Gallates of Megastigmane Glucosides, 3-hydroxyoctanoic Acid Glucosides and a Phenylpropanoid Glucoside from the Whole Plants of Euphorbia Hirta. *J. Nat. Med.* 67 (2), 350–358. doi:10.1007/s11418-012-0692-5

Nugroho, A., Heryani, H., and Istikowati, W. T. (2020). Quantitative Determination of Quercitrin and Myricitrin in Three Different Parts of Euphorbia Hirta as Bioflavonoid Source for Functional Food. *IOP Conf. Ser. Earth Environ. Sci.* 443, 012042–012046. doi:10.1088/1755-1315/443/1/012042

O'Boyle, N. M., Banck, M., James, C. A., Morley, C., Vandermeersch, T., and Hutchison, G. R. (2011). Open Babel: An Open Chemical Toolbox. *J. Cheminform* 3 (1), 33. doi:10.1186/1758-2946-3-33

Ogunlesi, M., Okiei, W., Ofor, E., and Osibote, A. E. (2009). Analysis of the Essential Oil from the Dried Leaves of Euphorbia Hirta Linn (Euphorbiaceae), a

Potential Medication for Asthma. *Afr. J. Biotechnol.* 8 (24), 7042–7050. doi:10.4314/AJB.V8I24.68792

Olaoluwa, O., Moronkola, D., Taiwo, O., and Iganboh, P. (2018). Volatile Oil Composition, Antioxidant and Antimicrobial Properties of Boerhavia Erecta L. And Euphorbia Hirta L. *Trends Phytochem. Res.* 2 (3), 171–178. Retrieved from: http://tpr.iau-shahrood.ac.ir/article_543327.html

Ortega, J. T., Suárez, A. I., Serrano, M. L., Baptista, J., Pujol, F. H., and Rangel, H. R. (2017). The Role of the Glycosyl Moiety of Myricetin Derivatives in Anti-HIV-1 Activity *In Vitro*. *AIDS Res. Ther.* 14 (1), 57. doi:10.1186/s12981-017-0183-6

Parvez, M. K., Al-Dosari, M. S., Arbab, A. H., Al-Rehaily, A. J., and Abdelwahid, M. A. S. (2020). Bioassay-Guided Isolation of Anti-Hepatitis B Virus Flavonoid Myricetin-3-O-Rhamnoside Along with Quercetin from Guiera Senegalensis Leaves. *Saudi Pharm. JournalThe Official Publ. Saudi Pharm. Soc.* 28 (5), 550–559. doi:10.1016/j.jsps.2020.03.006

Perera, S. D., Jayawardena, U. A., and Jayasinghe, C. D. (2018). Potential Use ofEuphorbia Hirtafor Dengue: A Systematic Review of Scientific Evidence. *J. Trop. Med.* 2018, 7. doi:10.1155/2018/2048530

Perumal, S., and Mahmud, R. (2013). Chemical Analysis, Inhibition of Biofilm Formation and Biofilm Eradication Potential of Euphorbia Hirta L. Against Clinical Isolates and Standard Strains. *BMC Complement. Altern. Med.* 13, 346. doi:10.1186/1472-6882-13-346

Perumal, S., Mahmud, R., and Mohamed, N. (2018). Combination of Epicatechin 3-Gallate from Euphorbia Hirta and Cefepime Promotes Potential Synergistic Eradication Action against Resistant Clinical Isolate of Pseudomonas aeruginosa. *Evidence-Based Complement. Altern. Med.* 2018, 1–7. doi:10.1155/2018/5713703

Perumal, S., Mahmud, R., and Ramanathan, S. (2015). Anti-Infective Potential of Caffeic Acid and Epicatechin 3-gallate Isolated from Methanol Extract ofEuphorbia hirta(L.) againstPseudomonas Aeruginosa. *Nat. Product. Res.* 29 (18), 1766–1769. doi:10.1080/14786419.2014.999242

Prachi, S., and Pradeep, T. (2014). 13α-methyl-27-norolean-14-en-3β-ol, a Triterpeneisolated from the Stem of *Euphorbia Hirta* (Linn) Possess an Anti-asthmatic Properties. *Res. J. Chem. Sci.* 4 (3), 21–26. Retrieved from: http://citeseerx.ist.psu.edu/viewdoc/download?doi=10.1.1.1082.2070andrep=rep1andtype=pdf

Ragasa, C. Y., and Cornelio, K. B. (2013). Triterpenes from Euphorbia Hirta and Their Cytotoxicity. *Chin. J. Nat. Medicines.* 11 (5), 528–533. doi:10.1016/S1875-5364(13)60096-5

Rao, C., Gupta, S., Azmi, L., and Mohapatra, P. (2017). Flavonoids from Whole Plant of Euphorbia Hirta and Their Evaluation against Experimentally Induced Gastroesophageal Reflux Disease in Rats. *Phcog Mag.* 13 (Suppl. 1), 127–S134. doi:10.4103/0973-1296.203987

Rautela, I., Joshi, P., Thapliyal, P., Pant, M., Dheer, P., Bisht, S., et al. (2020). Comparative GC-MS Analysis of *Euphorbia Hirta* and *Euphorbia Milli* for Therapeutic Potential Utilities. *Plant Arch.* 20 (2), 3515–3512. Retrieved from: http://plantarchives.org/20-2/3515-3522%20(6354).pdf

Reddy, B. U., Mullick, R., Kumar, A., Sharma, G., Bag, P., Roy, C. L., et al. (2018). A Natural Small Molecule Inhibitor Corilagin Blocks HCV Replication and Modulates Oxidative Stress to Reduce Liver Damage. *Antiviral Res.* 150, 47–59. doi:10.1016/j.antiviral.2017.12.004

Schwarz, S., Sauter, D., Wang, K., Zhang, R., Sun, B., Karioti, A., et al. (2014). Kaempferol Derivatives as Antiviral Drugs Against the 3a Channel Protein of Coronavirus. *Planta Med.* 80 (2–3), 177–182. doi:10.1055/s-0033-1360277

Selin-Rani, S., Senthil-Nathan, S., Thanigaivel, A., Vasantha-Srinivasan, P., Edwin, E.-S., Ponsankar, A., et al. (2016). Toxicity and Physiological Effect of Quercetin on Generalist Herbivore, Spodoptera Litura Fab. And a Non-Target Earthworm Eisenia fetida Savigny. *Chemosphere.* 165, 257–267. doi:10.1016/j.chemosphere.2016.08.136

Shah, A. P., Parmar, G. R., Sailor, G. U., and Seth, A. K. (2019). Antimalarial Phytochemicals Identification from Euphorbia Hirta against Plasmepsin Protease: An In Silico Approach. *Folia Med.* 61 (4), 584–593. doi:10.3897/folmed.61.e47965

Sharma, N., Samarakoon, K., Gyawali, R., Park, Y.-H., Lee, S.-J., Oh, S., et al. (2014). Evaluation of the Antioxidant, Anti-Inflammatory, and Anticancer Activities of Euphorbia Hirta Ethanolic Extract. *Molecules.* 19 (9), 14567–14581. doi:10.3390/molecules190914567

Sheliya, M. A., Rayhana, B., Ali, A., Pillai, K. K., Aeri, V., Sharma, M., et al. (2015). Inhibition of α-glucosidase by New Prenylated Flavonoids from euphorbia Hirta L. Herb. *J. Ethnopharmacology.* 176, 1–8. doi:10.1016/j.jep.2015.10.018

Shitrit, A., Zaidman, D., Kalid, O., Bloch, I., Doron, D., Yarnizky, T., et al. (2020). Conserved Interactions Required for Inhibition of the Main Protease of Severe Acute Respiratory Syndrome Coronavirus 2 (SARS-CoV-2). *Sci. Rep.* 10 (1), 20808. doi:10.1038/s41598-020-77794-5

Suganthi, A., and Ravi, T. K. (2018). Estimation of Anti-Dengue Phytochemical Markers Gallic Acid, Rutin and Quercetin in Methanolic Extract of Euphorbia Hirta (L.) and Tawa-Tawa Capsule Formulation by Validated RP-HPLC Method. *Chem. Methodologies.* 3 (1), 43–54. doi:10.22034/chemm.2018.129381.1051

Tawa-tawa Clinical Trial on COVID-19 (2021). Philippine Health Research Registry. Available at: https://registry.healthresearch.ph/index.php/registry?view=research&layout=details&cid=3475.

Tayone, W. C., Ishida, K., Goto, S., Tayone, J. C., Arakawa, M., Morita, E., et al. (2020). Anti-Japanese Encephalitis Virus (JEV) Activity of Triterpenes and Flavonoids from Euphorbia Hirta. *Philippine J. Sci.* 149 (3), 603–613. Retrieved from: https://philjournalsci.dost.gov.ph/publication/regular-issues/past-issues/98-vol-149-no-3-september-2020/1211-anti-japanese-encephalitis-virus-jev-activity-of-triterpenes-and-flavonoids-from-euphorbia-hirta

Trott, O., and Olson, A. J. (2009). AutoDock Vina: Improving the Speed and Accuracy of Docking with a New Scoring Function, Efficient Optimization, and Multithreading. *J. Comput. Chem.* 31 (2), 455–461. doi:10.1002/jcc.21334

Ullrich, S., and Nitsche, C. (2020). The SARS-CoV-2 Main Protease as Drug Target. *Bioorg. Med. Chem. Lett.* 30 (17), 127377. doi:10.1016/j.bmcl.2020.127377

Wang, S., Ling, Y., Yao, Y., Zheng, G., and Chen, W. (2020). Luteolin Inhibits Respiratory Syncytial Virus Replication by Regulating the MiR-155/SOCS1/STAT1 Signaling Pathway. *Virol. J.* 17 (1), 187. doi:10.1186/s12985-020-01451-6

Wang, Y. C., Yang, W. H., Yang, C. S., Hou, M. H., Tsai, C. L., Chou, Y. Z., et al. (2020). Structural Basis of SARS-CoV-2 Main Protease Inhibition by a Broad-Spectrum Anti-coronaviral Drug. *Am. J. Cancer Res.* 10 (8), 2535–2545. Retrieved from: https://www.ncbi.nlm.nih.gov/pmc/articles/PMC7471349/pdf/ajcr0010-2535.pdf

Wu, L.-l., Yang, X.-b., Huang, Z.-m., Liu, H.-z., and Wu, G.-x. (2007). *In Vivo* and *In Vitro* Antiviral Activity of Hyperoside Extracted from *Abelmoschus Manihot* (L) Medik. *Acta Pharmacologica Sinica.* 28 (3), 404–409. doi:10.1111/j.1745-7254.2007.00510.x

Wu, Y., Qu, W., Geng, D., Liang, J.-Y., and Luo, Y.-L. (2012). Phenols and Flavonoids from the Aerial Part of Euphorbia Hirta. *Chin. J. Nat. Medicines.* 10 (1), 40–42. doi:10.1016/S1875-5364(12)60009-0

Xu, H.-X., Wan, M., Dong, H., But, P. P.-H., and Foo, L. Y. (2000). Inhibitory Activity of Flavonoids and Tannins against HIV-1 Protease. *Biol. Pharm. Bull.* 23 (9), 1072–1076. doi:10.1248/bpb.23.1072

Yan, S., Ye, D., Wang, Y., Zhao, Y., Pu, J., Du, X., et al. (2011). Ent-Kaurane Diterpenoids from Euphorbia hirta. *Rec. Nat. Prod.* 5 (4), 247–251.

Yang, Z.-N., Su, B.-J., Wang, Y.-Q., Liao, H.-B., Chen, Z.-F., and Liang, D. (2020). Isolation, Absolute Configuration, and Biological Activities of Chebulic Acid and Brevifolincarboxylic Acid Derivatives from Euphorbia Hirta. *J. Nat. Prod.* 83 (4), 985–995. doi:10.1021/acs.jnatprod.9b00877

Zhang, L., Wang, X.-L., Wang, B., Zhang, L.-T., Gao, H.-M., Shen, T., et al. (2020). Lignans from Euphorbia Hirta L. *Nat. Product. Res.* 36, 26–36. doi:10.1080/14786419.2020.1761358

Zhu, L., Wang, P., Yuan, W., and Zhu, G. (2018). Kaempferol Inhibited Bovine Herpesvirus 1 Replication and LPS-Induced Inflammatory Response. *Acta Virologica.* 62 (2), 220–225. doi:10.4149/av_2018_206

Conflict of Interest: The authors declare that the research was conducted in the absence of any commercial or financial relationships that could be construed as a potential conflict of interest.

Publisher's Note: All claims expressed in this article are solely those of the authors and do not necessarily represent those of their affiliated organizations, or those of the publisher, the editors and the reviewers. Any product that may be evaluated in this article, or claim that may be made by its manufacturer, is not guaranteed or endorsed by the publisher.